

Article

Climate Change Impacts on Water Resources in Arid and Semi-Arid Regions: A Case Study in Saudi Arabia

Mustafa El-Rawy^{1,2,*} , Okke Batelaan³ , Nassir Al-Arifi^{4,*}, Ali Alotaibi², Fathy Abdalla^{5,6}  and Mohamed Elsayed Gabr⁷ 

¹ Civil Engineering Department, Faculty of Engineering, Minia University, Minia 61111, Egypt

² Civil Engineering Department, College of Engineering, Shaqra University, Dawadmi 11911, Saudi Arabia

³ National Centre for Groundwater Research and Training, College of Science and Engineering, Flinders University, GPO Box 2100, Adelaide, SA 5001, Australia

⁴ Chair of Natural Hazards and Mineral Resources, Geology and Geophysics Department, King Saud University, Riyadh 145111, Saudi Arabia

⁵ Deanship of Scientific Research, King Saud University, Riyadh 145111, Saudi Arabia

⁶ Geology Department, Faculty of Science, South Valley University, Qena 83523, Egypt

⁷ Civil Engineering Department, Higher Institute for Engineering and Technology, Ministry of High Education, New Damietta 34517, Egypt

* Correspondence: mustafa.elrawy@mu.edu.eg (M.E.-R.); nalarifi@ksu.edu.sa (N.A.-A.)

Abstract: In the coming years, climate change is predicted to impact irrigation water demand considerably, particularly in semi-arid regions. The aim of this research is to investigate the expected adverse impacts of climate change on water irrigation management in Saudi Arabia. We focus on the influence of climate change on irrigation water requirements in the Al Quassim (97,408 ha) region. Different climate models were used for the intermediate emission SSP2-4.5 and the high emission SSP5-8.5 Coupled Model Intercomparison Project Phase 6 (CMIP6) scenarios. The FAO-CROPWAT 8.0 model was used to calculate reference evapotranspiration (ET_o) using weather data from 13 stations from 1991 to 2020 and for both the SSP2-4.5 and SSP5-8.5 scenarios for the 2040s, 2060s, 2080s, and 2100s. The findings indicated that, for the 2100s, the SSP2-4.5 and SSP5-8.5 scenarios forecast annual average ET_o increases of 0.35 mm/d (6%) and 0.7 mm/d (12.0%), respectively. Net irrigation water requirement (NIWR) and growth of irrigation water requirement (GIWR) for the main crops in the Al Quassim region were assessed for the current, SSP2-4.5, and SSP5-8.5 scenarios. For SSP5-8.5, the GIWR for the 2040s, 2060s, 2080s, and 2100s are expected to increase by 2.7, 6.5, 8.5, and 12.4%, respectively, compared to the current scenario (1584.7 million m³). As a result, there will be higher deficits in 2100 under SSP5-8.5 for major crops, with deficits of 15.1%, 10.7%, 8.3%, 13.9%, and 10.7% in the crop areas of wheat, clover, maize, other vegetables, and dates, respectively. Optimal irrigation planning, crop pattern selection, and modern irrigation technologies, combined with the proposed NIWR values, can support water resources management. The findings can assist managers and policymakers in better identifying adaptation strategies for areas with similar climates.

Keywords: irrigation water demand; climate change; reference evapotranspiration; FAO-CROPWAT 8.0 model; CMIP6



Citation: El-Rawy, M.; Batelaan, O.; Al-Arifi, N.; Alotaibi, A.; Abdalla, F.; Gabr, M.E. Climate Change Impacts on Water Resources in Arid and Semi-Arid Regions: A Case Study in Saudi Arabia. *Water* **2023**, *15*, 606. <https://doi.org/10.3390/w15030606>

Academic Editor: Micòl Mastrocicco

Received: 17 December 2022

Revised: 24 January 2023

Accepted: 29 January 2023

Published: 3 February 2023



Copyright: © 2023 by the authors. Licensee MDPI, Basel, Switzerland. This article is an open access article distributed under the terms and conditions of the Creative Commons Attribution (CC BY) license (<https://creativecommons.org/licenses/by/4.0/>).

1. Introduction

Climate change is one of the most challenging environmental concerns for development because of its impact on water security, especially in arid and semi-arid regions. Increased evapotranspiration from agriculture is anticipated in the coming years due to the expected changes in temperature, precipitation intensity, annual amount, temporal distribution, atmospheric water vapor, and soil water content. This will significantly impact irrigation water requirements, especially in semi-arid areas [1]. Understanding how climate change affects crop water requirements (CWR) is crucial for addressing future food security and water resource sustainability challenges [2–4].

General Circulation Model (GCM) simulations as part of Coupled Model Intercomparison Project (CMIP) are essential for providing quantitative climate projections for the twenty-first century [5]. The fourth Intergovernmental Panel on Climate Change (IPCC) assessment report was created using the CMIP phase 3 (CMIP3) GCM simulations [6]. The fifth assessment report (AR5) of the IPCC was created using the CMIP5 [7]. In terms of physical processes and network precision, the CMIP5 models were improved over the CMIP3 models [8]. When the CMIP3 and CMIP5 models were compared, CMIP5 GCMs performed better at mimicking the observed climate in many locations and the large-scale air circulations that control regional climates [9]. Climate scenarios are provided for four representative concentration pathways (RCPs), namely RCP 2.6, RCP 4.5, RCP 6, and RCP 8.5, up to 2100 [7]. Researchers [9–12] have used RCP scenarios to simulate how climate change affected water resources globally over the last decade, showing a significant impact.

Phase 6 of the CMIP has recently published a fresh coordinated set of climate experiments [13]. The CMIP6 GCMs differ from past generations in a number of ways, including improved cloud microphysics, higher geographic resolutions, and improved earth system processes and components, such as ice sheets and biogeochemical cycles [14]. The scenarios for the future are the key distinctions between CMIP5 and CMIP6. Four GHG concentration paths have accessible CMIP5 forecasts based on radiative forcing values for the year 2100 [15].

Gusain et al. [16] investigated the effectiveness of CMIP6 and CMIP5 models in simulating summer rainfall in India and found inconsistent added value. They assert that the additional value in CMIP6 models' simulations of precipitation is inconsistent across the climate models employed in the current analysis. The scientific community can still use it as a model for future research on assessing the effects of climate change. According to Nie et al. [17], CMIP6 models provide more precise estimates of the amplitude of global temperature extremes than CMIP5. The greater ability of the CMIP6 models to simulate decreasing precipitation and droughts in Southwestern South America was demonstrated by Rivera and Arnould [18].

In their analysis of the CMIP6 global climate models (GCMs), Mohammad et al. [19] found that the Australian Community Climate and Earth-System Simulator (ACCESS-CM2) and the Atmosphere and Ocean Research Institute (Tokyo University), National Institute for Environmental Studies, and Japan Agency for Marine-Earth Science and Technology, Japan (MIROC5) models performed best at simulating Bangladesh's annual and seasonal rainfall and temperature. Additionally, they discovered that the modeling of rainfall and temperature across Bangladesh by the CMIP6 multi-model ensemble (MME) demonstrated a significant improvement over the CMIP5 MME. As a function of climatic variables such as temperature and precipitation under various RCPs scenarios, several researchers evaluated the changes in ETo and CWR [20,21].

Expected increases in temperature and precipitation extremes were used to analyze changes in (ETo) and regional agricultural water demand in China's Hetao Irrigation District; an increase of 4% to 7% in future ETo levels was shown [22]. The effects of climate change on crop water requirements in Saudi Arabia's Al-Jouf (desert area) in 2050 were examined by [4]. They estimated that the demand for agricultural water would rise by 2.9% for every 1 °C rise in temperature. Tarawneh and Chowdhury [23] looked into how Saudi Arabia's water supplies might be affected by trends of climate change. They assessed three emission scenarios (RCP8.5, RCP6, and RCP 2.6) for the assessment periods of 2025–2044, 2045–2064, and 2065–2084, respectively, and compared the average values to the outputs of the NCAR Community Climate System Model for the reference period (1986–2005). They concluded that from 1986 to 2005, the temperature in all regions rose for all emission scenarios. The temperature rises between 2025 and 2044, between 2045 and 2064, and between 2065 and 2084 with RCP8.5 are predicted to be in the ranges of 0.8–1.6 °C, 0.9–2.7 °C, and 0.7–4.1 °C.

Different climate models were utilized by Moghazy and Kaluarachchi [24] for RCP 4.5 and RCP 8.5 for years 2060 and 2100 in the Siwa region located in the Western Desert

of Egypt for a project in which 30,000 acres will be reclaimed to increase agricultural production. The increase in agricultural water requirements is predicted to be between 6 and 8.1% for RCP 4.5 and between 9.7 and 18.2% for RCP 8.5. Maximum reductions in strategic crop yield under RCP 4.5 range from 2.9% to 12.8% in 2060, but maximum reductions under RCP 8.5 range from 10.4% to 27.45 in 2100. Using the RCP 2.6, RCP 4.5, RCP 6, and RCP 8.5 for the years 2011–2040, 2041–2070, and 2071–2100, Abdrabbo et al. [25] examined ETo in Egypt, which, compared to the current ETo, is expected to increase by roughly 5% to 20.1% in the Delta region and 4.7% to 19.65 in central Egypt. The increase in ETo in the south of Egypt might be from 11% to 26.8%.

The Penman–Monteith method [26] is recommended as an internationally standard approach for quantifying reference crop evapotranspiration, ETo. Therefore, many studies have used the Penman–Monteith–FAO ETo approach [27]. On the other hand, other approaches to calculating ETo were used [13,28,29] depending on the information at hand, including methods based on mass transfer, radiation, and temperature. The Penman–Monteith equation served as the foundation for Smith’s [30] creation of the CROPWAT 8.0 modeling program, which is widely used in the global water management sector.

The FAO Land and Water Division created AquaCrop [31], a crop growth model, to address food security and evaluate how the environment and management affect crop productivity. AquaCrop models how herbaceous crops respond in terms of yield to water and is especially well adapted to situations where water is a major production-limiting factor. Accuracy, simplicity, and robustness are all balanced by AquaCrop. It simply utilizes a small number of explicit parameters and generally sensible input variables that can be determined using straightforward methods, ensuring its broad application.

The objectives of this study are to use multiple prediction climate models to investigate the expected negative impacts of climate change over Saudi Arabia, as well as their impact on irrigation water management in the Al Quassim region, which is one of Saudi Arabia’s most important agricultural areas. The ETo and net irrigation water requirement (NIWR) for the most important cultivated crops were calculated using the FAO CROPWAT 8.0 model [30]. The study of demand changes can benefit both irrigation planning and future modeling of groundwater aquifer.

To accomplish this goal, (i) the meteorological data of 13 climatic stations located in Saudi Arabia are collected from 1991 to 2020; (ii) the future climate model data from the CMIP6 database under SSP2-4.5 and SSP5-8.5 for 2040, 2060, 2080, and 2100 are collected; (iii) the Penman–Monteith method for estimating ETo was used as implemented in the FAO-CROPWAT 8.0 model [30]; (iv) using GIS (a geographic information system), T_{max} (maximum temperatures), T_{min} (minimum temperatures), rainfall, and ETo, maps for Saudi Arabia were produced for the current climate and for the SSP2-4.5 and SSP5-8.5; (v) the net irrigation water requirements (NIWR) for the major crops in Al Quassim region were estimated for the current, SSP2-4.5 and SSP5-8.5 emission scenarios; (vi) the deficits in the crop areas of the main crops in Al Quassim region were estimated for the SSP2-4.5 and SSP5-8.5 emission scenarios.

2. Materials and Methods

2.1. Description of the Study Area

Saudi Arabia is located within the boundaries of latitudes 16°30′ N and 32°30′ N and longitudes 33°45′ E and 55°40′ E (Figure 1a). Because of its arid climate, Saudi Arabia has hot, dry summers and cool, slightly humid winters [23]. In the summer and winter, the maximum monthly average temperature ranges between 30 and 44 °C and between 15 and 28 °C, respectively. Because the majority of the country experiences a range of climatic conditions between summer and winter, climatic elements differ from region to region and even within the same region. In July, temperatures in Al Riyadh, Hafr Al-Baten, Al Quassim, Al Hassa, and other central and eastern cities regularly reach 45 °C, while the highlands remain cooler, with maximum temperatures not exceeding 30 °C (e.g., Asser and Al-Baha). Most of the country has very low relative humidity, especially in the summer.

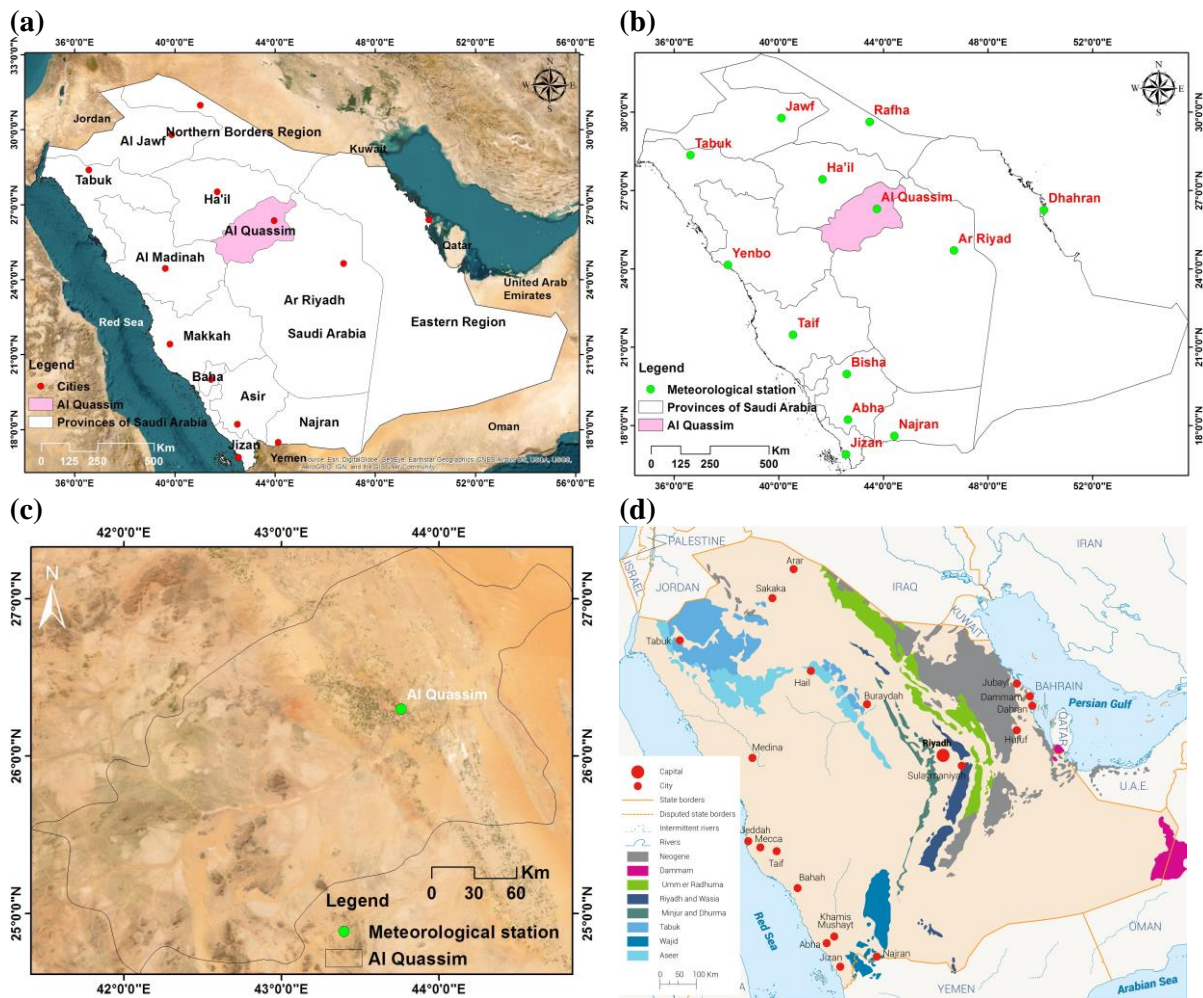


Figure 1. (a) Provinces of Saudi Arabia, (b) meteorological stations in Saudi Arabia, (c) the Al Quassim region, and (d) main aquifers in Saudi Arabia [Ministry of Environment, Water and Agriculture, 2018. National Water Strategy 2030].

The average annual rainfall is below 150 mm, with the exception of the southwest, where it ranges between 400 and 600 mm [32] and potential evaporation is extremely high. Surface water (rainfall), groundwater (renewable and non-renewable), desalination water, and treated wastewater are the four categories of water resources in the country [33].

The Arabian Shelf is home to significant groundwater resources in both non-renewable aquifers and renewable alluvial aquifers [34,35]. Figure 2d shows the aquifers of Neogene, Dammam, Umm er Radhuma, Riyadh and Wasia, Tabuk, Wajid, and Aseer [36]. Al-Sheikh [37] estimated that the non-renewable aquifers have 259.1, 415.6, and 760.6 km³ of confirmed, probable, and potential groundwater reserves, respectively.

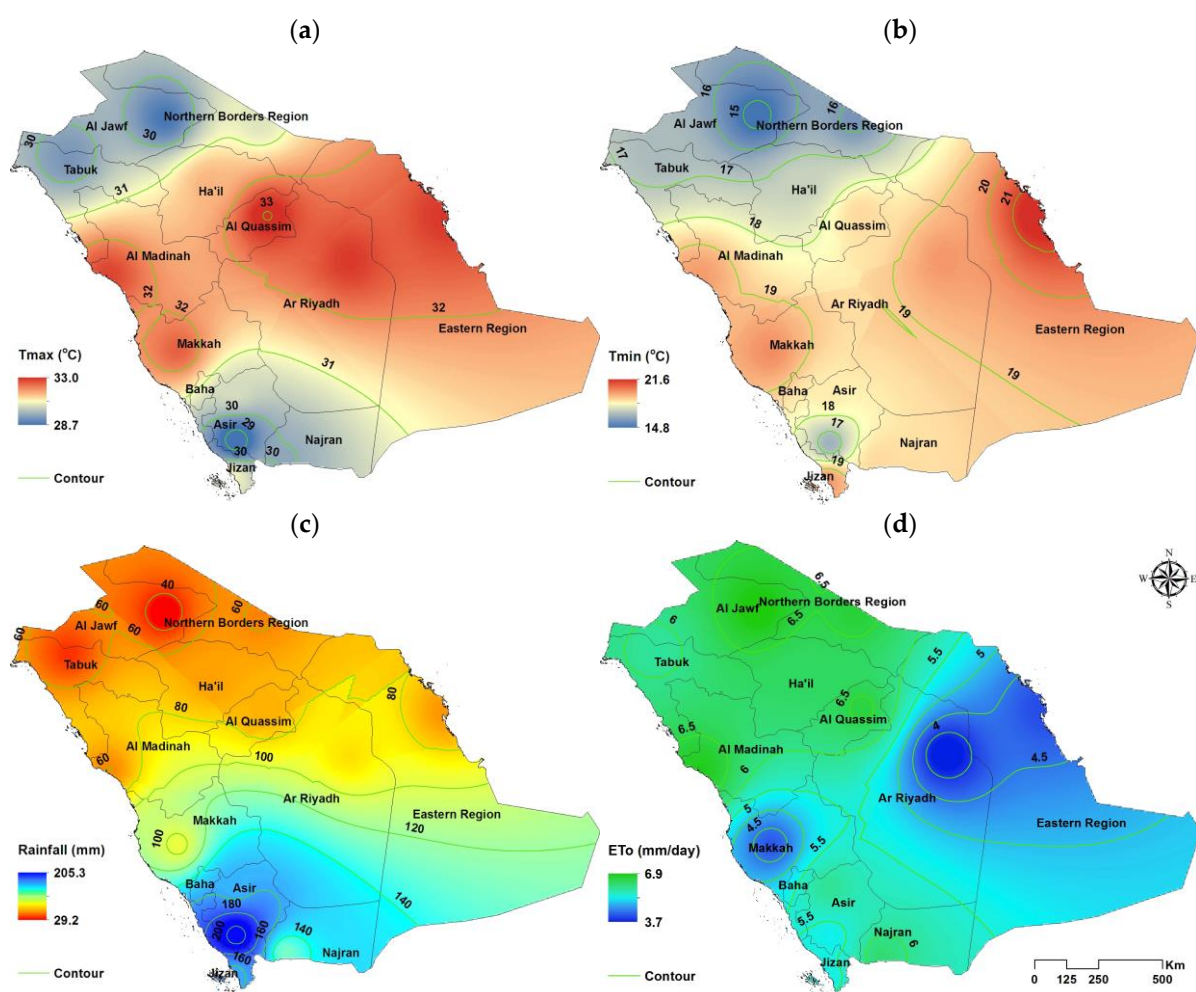


Figure 2. (a) Maximum and (b) minimum temperature ($^{\circ}\text{C}$), (c) rainfall (mm), and (d) reference evapotranspiration (ET_0) (mm) for 1991–2020.

The Al Qassim region, as one of Saudi Arabia's most important agricultural areas (97,408 ha), is situated between $24^{\circ}70' \text{ N}$ and $27^{\circ}20' \text{ N}$ and between $41^{\circ}25' \text{ E}$ and $44^{\circ}50' \text{ E}$ (Figure 1c). Groundwater from the Saq Aquifer [38] is the main source of water for the Al Qassim region.

2.2. Meteorological Data

The CMIP6 database is used to obtain the climate model data. (<https://pcmdi.llnl.gov/CMIP6/> (accessed on 4 January 2022)). This study used four CMIP6 models, as presented in Table 1: the CSIRO and ARCCSS model (ACCESS-CM2); 2: the Beijing Climate Center model (BCC-CSM2-MR); 3: the Centre National de Recherches Meteorologiques model (CNRM-CM6-1); and 4: the Meteorological Research Institute model (MRI-ESM2-0). The horizontal resolutions of the CMIP6 models vary; the CMIP6 data sets are regridded from their original spatial resolutions to a grid resolution, as mentioned in Table 1. Standard bilinear interpolation is used to regrid temperature data, while a first-order conservative method is used to regrid precipitation data [39].

Table 1. Characteristics of the four CMIP6 climate models utilized in the study.

Model No.	Multi-Model Ensemble	Country	Model Center	Responsible INSTITUTION	Resolution (Lon × Lat)	Ensemble Member	Key Reference
M1	ACCESS-CM2	Australia	CSIRO-ARCCSS	CSIRO (Commonwealth Scientific and Industrial Research Organization, Australia), and ARCCSS (Australian Research Council Centre of Excellence for Climate System Science)	1.9° × 1.3°	r1i1p1f1	[40]
M2	BCC-CSM2-MR	China	BCC	Beijing Climate Center	1.1° × 1.1°	r1i1p1f1	[41]
M3	CNRM-CM6-1	France	CNRM	Centre National de Recherches Meteorologiques	1.4° × 1.4°	r1i1p1f2	[42]
M4	MRI-ESM2-0	Japan	MRI	Meteorological Research Institute	1.1° × 1.1°	r1i1p1f1	[43]

Future estimated ETo values should be based on climate projections for two future Shared Socioeconomic Pathways (SSPs): SSP2-4.5 (Medium-low emissions) and SSP5-8.5 (High emissions), up to 2100. The selection of these models, however, was based on the availability of the meteorological data: maximum temperature (Tmax), minimum temperature (Tmin), and rainfall were used for future climate projections under SSP2-4.5 and SSP5-8.5 for the years 2040, 2060, 2080, and 2100.

FAO-CROPWAT 8.0 used as input meteorological data wind speed (km/h), Tmax and Tmin (°C), rainfall (mm), mean relative humidity, and sunshine hours (h) for 13 climatic stations located in Saudi Arabia (Figure 1b). The selected stations have climate data from 1991 to 2020. The locations and heights of the 13 climatic stations and the average meteorological parameters and calculated ETo for the 13 stations from 1991 to 2020 are shown in Table 2. The meteorological parameters from 1991 to 2020 are utilized as a reference base (current case) of this study.

Table 2. Coordinates, altitude and average climatic parameters for the 13 stations between 1991 and 2020 in Saudi Arabia.

Station Name	Altitude (m)	Latitude (N°)	Longitude (E°)	Min. Temp. (°C)	Max. Temp. (°C)	Relative Humidity (%)	Wind Speed (km/day)	Sunshine (Hours)	Solar Radiation (MJ/m ² /day)	Rainfall (mm)	ETo (mm/day)
Al Jawf	689	29.78	40.1	15.8	28.3	29	324	8.4	19	58	6.93
Baha (Bisha)	1163	19.98	42.61	16.9	32.1	29	209	7.7	19.3	124	5.96
Eastern Region (Dhahran)	17	26.26	50.15	20.3	32.2	50	79	7.3	18	79	4.16
Al Quassim	650	26.3	43.76	16.5	31.4	30	238	8.1	19.1	183	6.57
Gizan	3	16.9	42.58	26.1	34.5	65	317	7.7	19.6	104	5.45
Northern Borders Region (Rafha)	447	29.63	43.48	15.8	30.7	33	284	8.4	19	69	6.62
Ha'il	1013	27.43	41.68	13.7	28.3	33	248	8.4	19.4	171	6.32
Al Madinah (Yenbo)	6	24.15	38.06	20.1	32.4	59	432	8.4	19.8	97	6.8
Najran	1210	17.61	44.43	16.2	32.1	25	220	7.7	19.6	136	6.2
Ar Riyadh	612	24.71	46.71	18.6	32.7	30	42	7.9	19.1	101.3	3.66
Asir (Abha)	2093	18.23	42.65	11.9	24.7	56	320	7.3	18.9	272	5.38
Tabuk	776	28.36	36.63	13.6	28.9	32	230	7.8	18.4	58	5.92
Makkah (Taif)	1454	21.48	40.55	15.7	29.1	31	61	8.6	20.4	119	4.26

A geographic information system (ArcGIS) (<https://www.esri.com/en-us/arcgis/products/arcgis-pro/resources> (accessed on 13 April 2022)) as an efficient mapping tool was used to generate spatially distributed maps of meteorological data and ETo for Saudi Arabia. All the meteorological data and ETo results have been interpolated using Inverse Weighted Distance in GIS.

2.3. Soil and Crop Data

The Al Quassim region's crop water requirements (CWR) were investigated using soil and crop data from different crops (wheat, sorghum, maize, barley, tomato, potato, other vegetables, clover, dates, citrus, and grapes) [44,45]. Crop and soil data, first and last planting dates, first and last harvesting dates, irrigation practices used, length of plant growing season, and rooting depth were collected using field observations and conversations with farmers [44,45]. In the Al Quassim region, medium soil is the most common (sandy loam). Table 3 shows the soil parameters of the Al Quassim region, as well as crop planting and harvesting dates.

Table 3. Soil parameters and crop planting and harvesting dates for the Al Quassim region.

Al Quassim Region			
	No.	Soil Parameter	Value
Medium soil (sandy loam)	1	Total available soil moisture (Field capacity-Wilting point)	200 mm m ⁻¹
	2	Maximum infiltration rate	40 mm day ⁻¹
	3	Maximum rooting depth	250 cm
	4	Initial soil moisture depletion	0%
	5	Initial available soil moisture	190 mm m ⁻¹
Crop data (planting, harvest dates, and cultivated area)			
Crop	Planting date	Harvest date	Cultivated area (ha)
Wheat	15-Jan.	24-May	22,792
Maize	1-Apr.	3-Aug.	5983
Barley	1-Nov.	28-Feb.	55
Tomato	1-Apr.	23-Aug.	920
Potato	15-Jan.	24-May	3826
Other vegetables	1-Mar.	3-Jun.	6671
Clover	1-Dec.	30-Nov.	14,786
Dates	1-Apr.	3-Aug.	39,303
Citrus	1-Mar.	28-Feb.	2014
Grapes	1-Apr.	31-Mar.	1058
Total			97,408

2.4. CROPWAT 8 Model

CROPWAT 8.0 is developed by the FAO that can estimate ET_0 , CWR, net and growth irrigation water requirement (NIWR, and GIWR), and irrigation schedule using rainfall, soil, crop, and climatic data.

The FAO Penman–Monteith equation for computing ET_0 [26] is:

$$ET_0 = \frac{0.408\Delta(R_n - G) + \gamma u_2 \frac{900}{T+273}(e_s - e_a)}{\Delta + \gamma(1 + 0.34 u_2)} \quad (1)$$

where ET_0 : reference evapotranspiration (mm day⁻¹); R_n : net Radiation (MJ m⁻² day⁻¹); G : soil heat flux density (MJ m⁻² day⁻¹); T : mean daily air temperature at 2 m height (°C); u_2 : wind speed at 2 m height (m s⁻¹); e_s : saturation vapor pressure (kPa); e_a : actual vapor pressure (kPa); $e_s - e_a$: saturation vapor pressure deficit (kPa); Δ : slope of vapor pressure curve (kPa °C⁻¹); γ : psychrometric constant (kPa °C⁻¹).

ET_0 is the main parameter used to calculate crop evapotranspiration (ET_c), equation 2. ET_c was computed as the product of ET_0 and the crop coefficient (K_c). The ET_c value was

calculated using ET_o from Equation (1), and crop coefficient (K_c) values have been obtained from FAO irrigation and drainage paper [26]:

$$ET_c = K_c \times ET_o \tag{2}$$

The NIWR and GIWR were computed by the following two equations:

$$NIWR = ET_c - R_{eff} \tag{3}$$

$$GIWR = \frac{NIWR}{\eta} \tag{4}$$

where η is irrigation efficiency, which varies depending on the irrigation method, and R_{eff} is effective rainfall (mm), which can be determined by the dependable rainfall (FAO/AGLW formula) [26]:

$$R_{eff} = 0.6P - 10 \text{ for } P_{\text{month}} \leq 70 \text{ mm} \tag{5}$$

where P_{month} is rainfall intensity (mm/month).

3. Results

3.1. Temperature Distribution and Change

Figure 2a,b depicts the spatially distributed mean T_{min} and T_{max} for Saudi Arabia from 1991 to 2020. T_{min} ranges from 14.8 to 21.6 °C, with a spatial average of 18.3 °C. T_{max} ranges between 28.7 and 33.0 °C, with a spatial average of 31.2 °C. Figure 2c,d will be discussed in Sections 3.2 and 3.3, respectively.

The projected climate scenarios for 13 locations in Saudi Arabia using the four CMIP6 climate models were generated using the SSP2-4.5 and SSP5-8.5 for four periods: 2040, 2060, 2080, and 2100 (Table 4).

Table 4. Minimum and maximum temperatures (°C) and rainfall (mm) (average, range, difference, and change) using the four CMIP6 climate models for the four periods (2040, 2060, 2080, and 2100) under SSP2-4.5 and SSP5-8.5 and current conditions (2020).

		Tmin (°C)				
		Current (2020)	2040	2060	2080	2100
SSP2-4.5	Average	18.3	20.0	20.7	21.3	21.8
	Range	14.8–21.6	14.7–27.7	15.2–28.3	16.0–28.7	16.3–29.0
	ΔT	-	1.8	2.4	3.0	3.5
	Change (%)	-	10	13	17	19
SSP5-8.5	Average	18.3	20.3	21.5	22.9	24.4
	Range	14.8–21.6	14.8–27.8	15.9–28.6	17.3–29.7	19.0–30.8
	ΔT	-	2.1	3.3	4.6	6.2
	Change (%)	-	11	18	25	34
		Tmax (°C)				
SSP2-4.5	Average	31.2	31.4	31.8	32.3	32.8
	Range	28.7–33.0	28.3–33.7	29.1–34.5	29.5–35.1	30.3–35.4
	ΔT	-	0.2	0.7	1.2	1.6
	Change (%)	-	1	2	4	5
SSP5-8.5	Average	31.2	31.4	32.6	33.9	35.2
	Range	28.7–33.0	28.4–34.6	29.7–35.7	31.2–37.0	32.6–38.4
	ΔT	-	0.3	1.4	2.7	4.1
	Change (%)	-	1	5	9	13
		Rainfall (mm)				
SSP2-4.5	Average	93.2	108.1	102.6	104.1	118.7
	Range	29.2–205.3	47.8–176.5	40.8–168.7	43.0–172.3	48.6–200.8
	Δ Rainfall	-	14.9	9.4	10.9	25.5
	Change (%)	-	16	10	12	27
SSP5-8.5	Average	93.2	108.7	106.9	106.7	122.8
	Range	29.2–205.3	51.0–167.2	51.1–177.4	43.4–181.6	51.7–205.1
	Δ Rainfall	-	15.5	13.7	13.5	29.6
	Change (%)	-	17	15	15	32

Minimum temperatures are 18.3, 20, 20.7, 21.3, and 21.8 (°C) in the current case (2020) and SSP2-4.5 in 2040, 2060, 2080, and 2100, respectively. This represents an increase of 1.8, 2.4, 3, and 3.5% over the current situation. Maximum temperatures for 2020 are 31.2, 31.4, 31.8, 32.3, and 32.8 (°C) with SSP2-4.5 for 2040, 2060, 2080, and 2100, respectively. This represents increases of 1, 2, 4, and 5%.

Minimum temperatures are 18.3, 20.3, 21.5, 22.9, and 24.4 °C for 2020 and SSP5-8.5 in 2040, 2060, 2080, and 2100, respectively. This indicates an increase of 11, 18, 25, and 34% compared to the current. Maximum temperatures are 31.2, 31.4, 32.6, 33.9, and 35.2 °C for 2020 and SSP5-8.5 in 2040, 2060, 2080, and 2100, respectively. This indicates an increase of 1, 5, 9, and 13% compared to the current case.

Figures 3 and 4 show the spatial distribution of the projected mean monthly Tmin and Tmax for the 2040, 2060, 2080, and 2100 under the SSP2-4.5 and SSP5-8.5 scenarios based on the four CMIP6 climate models. In both scenarios, Tmin and Tmax showed an increasing trend.

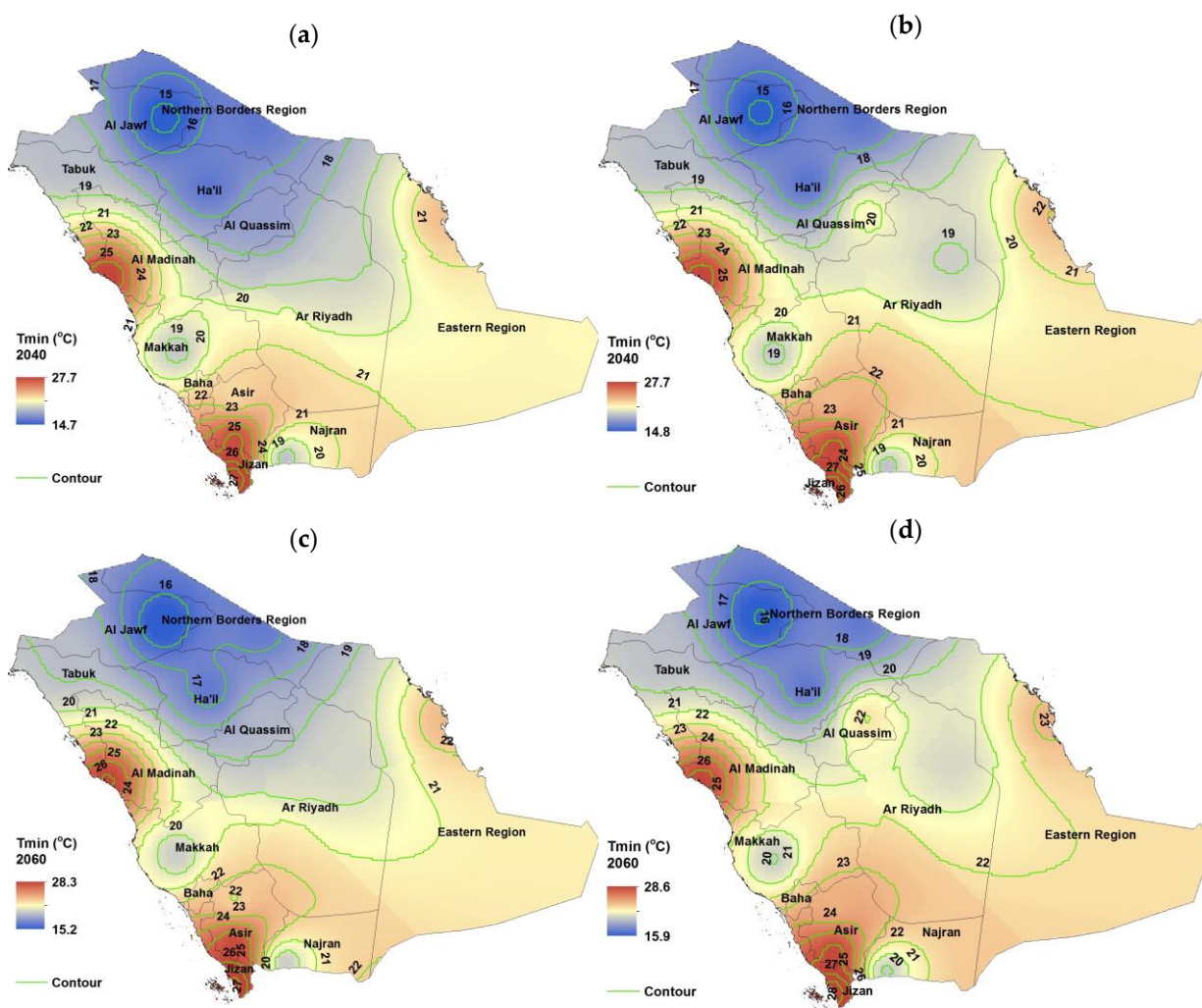


Figure 3. Cont.

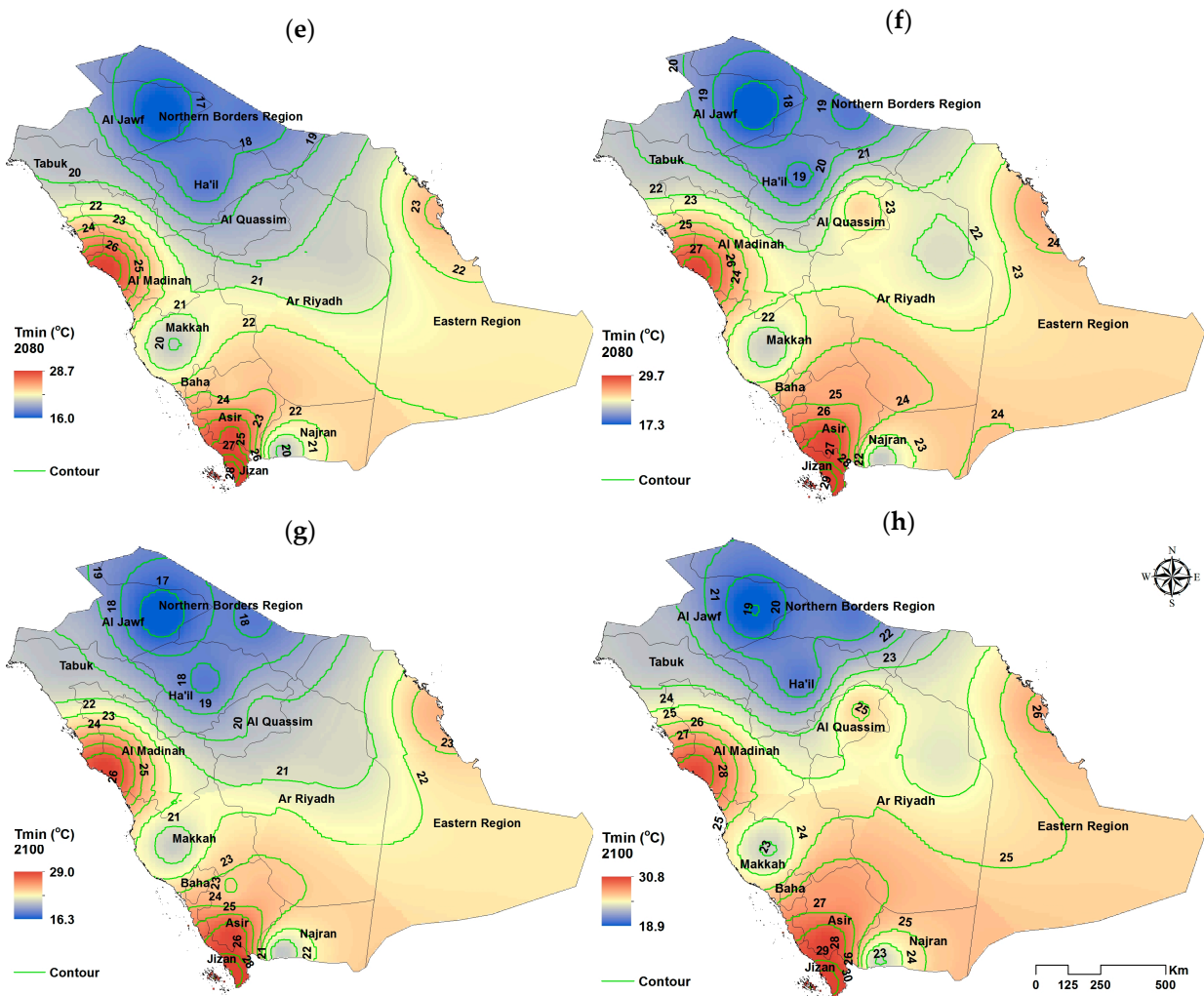


Figure 3. Annual-averaged Tmin (°C) under SSP2-4.5 on the left for (a) 2040, (c) 2060, (e) 2080, and (g) 2100 and SSP2-8.5 on the right for (b) 2040, (d) 2060, (f) 2080, and (h) 2100.

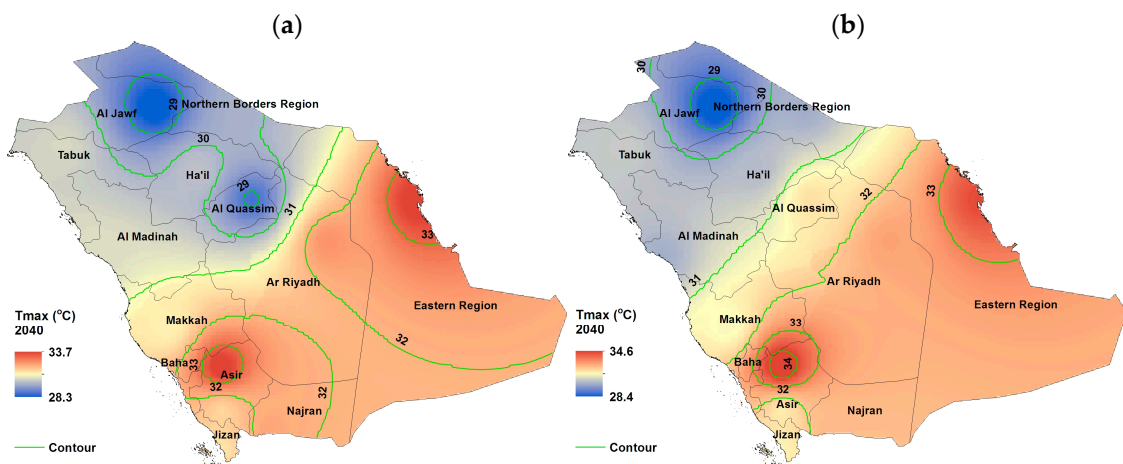


Figure 4. Cont.

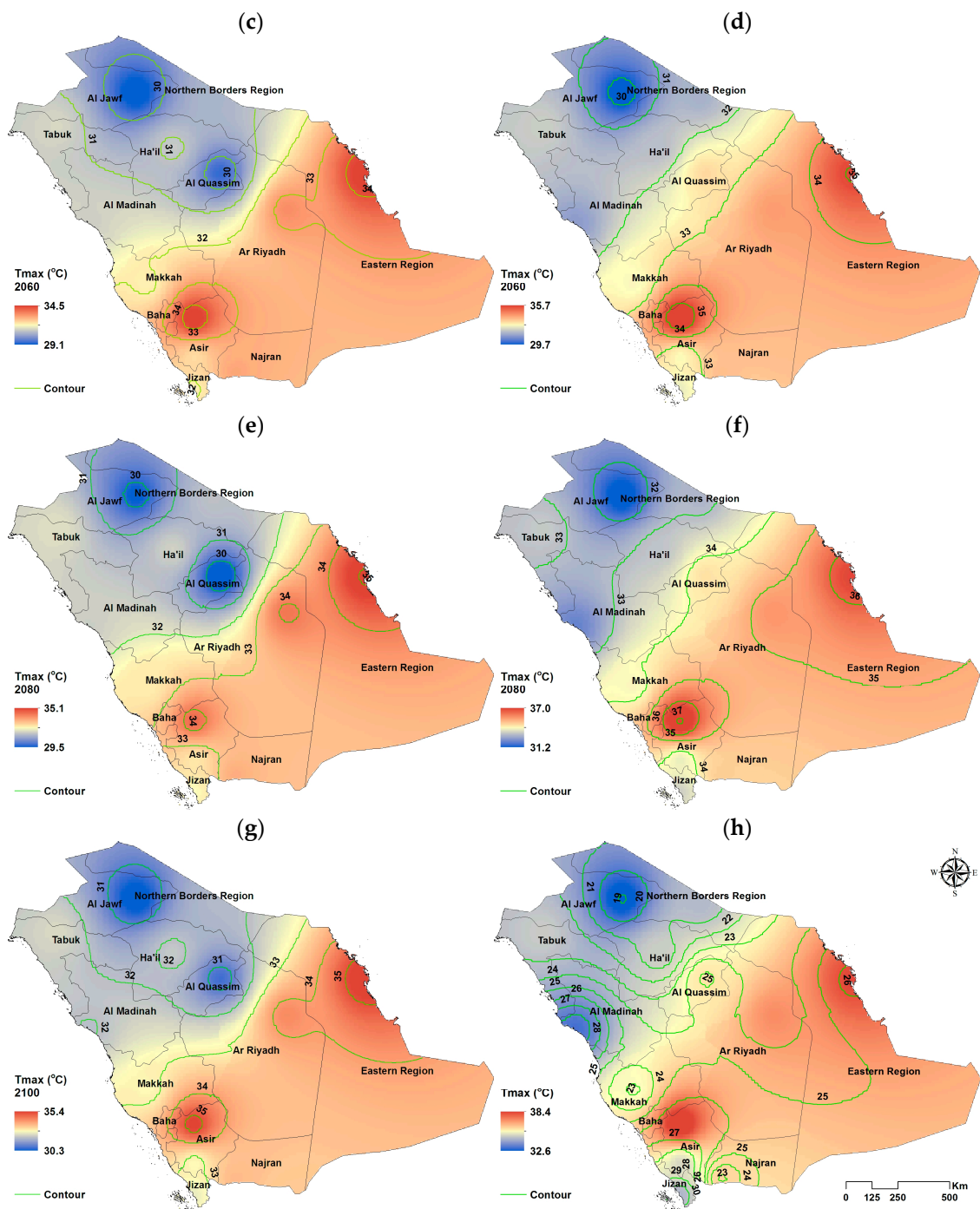


Figure 4. Annual-averaged Tmax (°C) under SSP2-4.5 on the left for (a) 2040, (c) 2060, (e) 2080, and (g) 2100 and SSP2-8.5 on the right for (b) 2040, (d) 2060, (f) 2080, and (h) 2100.

Under the SSP2-4.5 and SSP5-8.5 scenarios, Tmin will rise 10% and 11% in the 2040s, respectively, with Tmax rising 1.0% in both. Tmin will increase by 19% and 34% in the 2100s, respectively, under the SSP2-4.5 and SSP5-8.5 scenarios, and Tmax will increase by 5% and 13%, respectively, in comparison to the current scenario (2020) (Table 4). As a result, Tmax will rise by 0.18% (0.05 °C) per year from 2020 to 2100 under SSP5-85 (Table 4). The highest maximum temperature is expected to be observed in the Al Quassim region and extend to the eastern border under all SSP2-4.5 and SSP5-8.5 scenarios, as revealed in Figures 3 and 4.

3.2. Rainfall Distribution and Change

Figure 2c shows the spatially distributed precipitation for 1991–2020, where the spatial average is 93.2 mm. The rainfall ranges from 29.2 to 205.3 mm, with the highest values in the western- southern regions (Figure 2c). The projected mean annual rainfall distribution maps for Saudi Arabia under the SSP2-4.5 and SSP5-8.5 scenarios for the 2040s, the 2060s, the 2080s, and 2100s based on the four CMIP6 climate models are displayed in Figure 5.

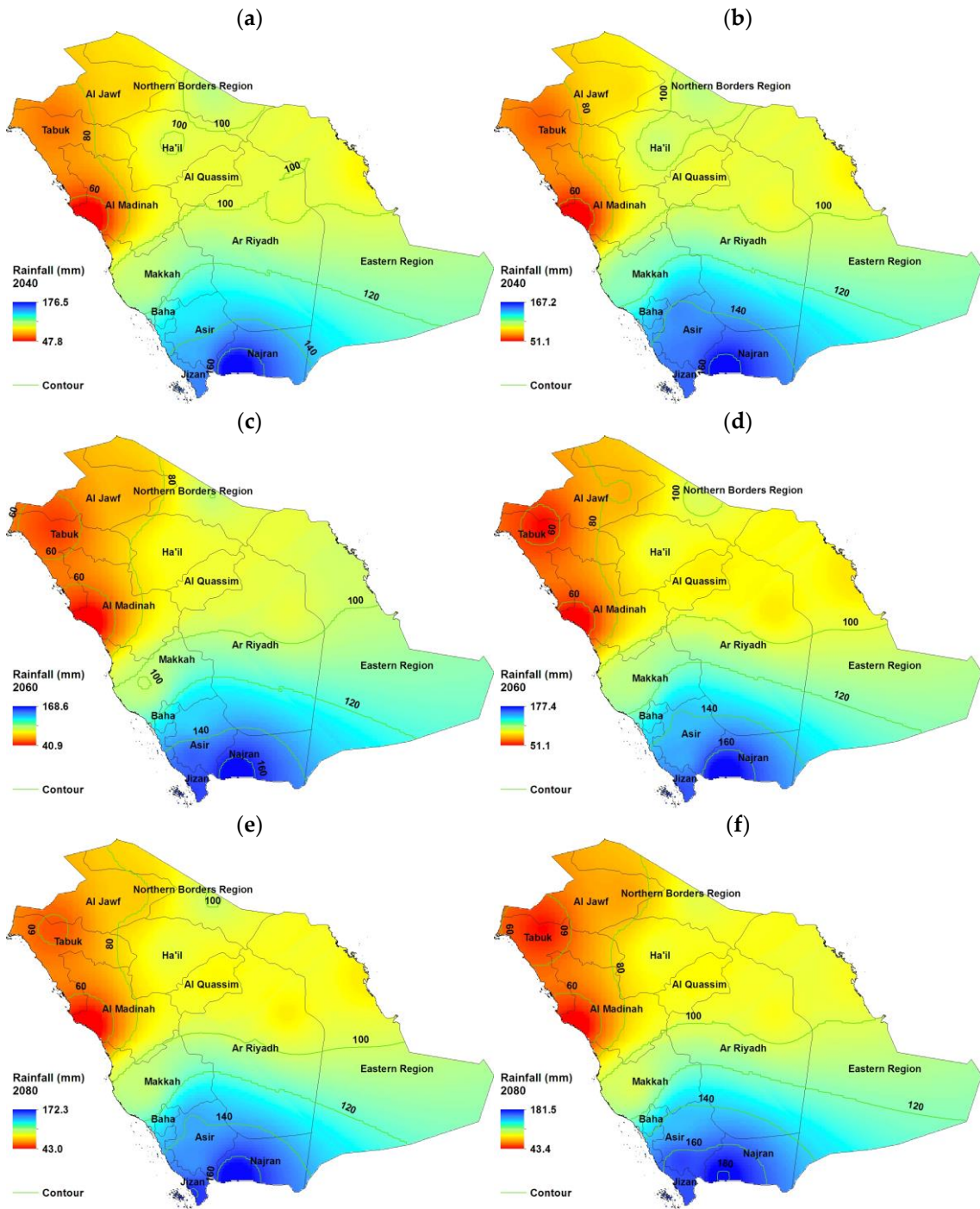


Figure 5. Cont.

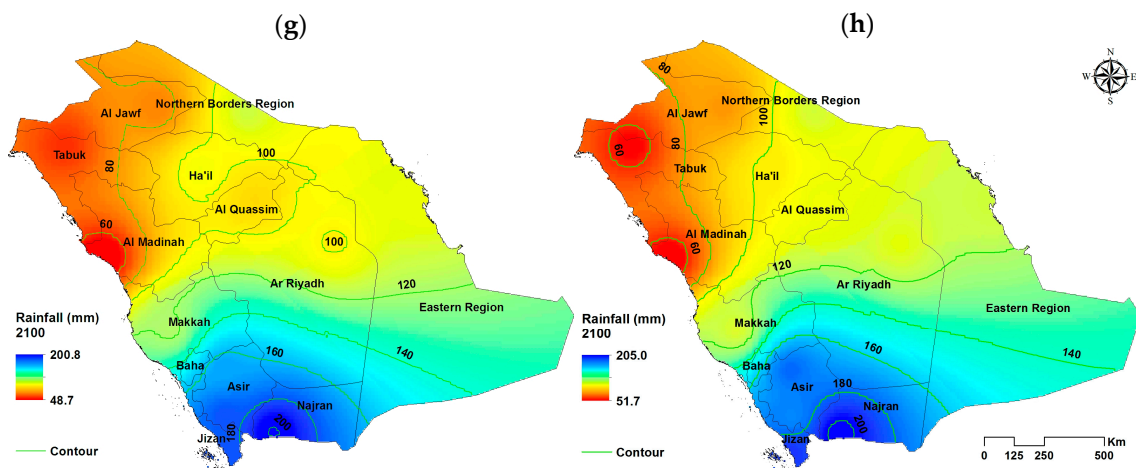


Figure 5. Annual-averaged rainfall (mm) SSP2-4.5 on the left for (a) 2040, (c) 2060, (e) 2080, and (g) 2100 and SSP2-8.5 on the right for (b) 2040, (d) 2060, (f) 2080, and (h) 2100.3.3. Reference Evapotranspiration Distribution and Change.

Under the SSP2-4.5 and SSP5-8.5 scenarios, annual average rainfall will increase by 14.9 mm and 15.5 mm, respectively, indicating an increasing ratio of 16% and 17% in the 2040s. For the 2100s, the annual average rainfall will increase by 25.5 mm and 29.6 mm, respectively, indicating an increasing ratio of 27% and 32%, respectively, compared to the current scenario (Table 4). As a result, the average rainfall will increase by 0.4 mm per year from 2020 to 2100 under SSP5-8.5 scenario (Table 4).

Figure 2d shows the distribution map for the estimated ETo in mm/day calculated by the CROPWAT 8 model. The ETo ranges from 3.7 to 6.9 mm/day with an average of 5.71 mm/day. For both the SSP2-4.5 and SSP5-8.5 scenarios, the simulated climatic parameters were incorporated into the CROPWAT model, and future ETo values were computed. Figure 6 demonstrates Saudi Arabia’s average daily ETo (mm/day) distribution maps using average data from the four CMIP6 climate models, with current conditions (2020) for the 13 stations. For both SSPs scenarios, the ETo measurements revealed an increasing tendency in the future.

Annual ETo increases by 2%, 4%, 5%, and 6% under the SSP2-4.5 scenario in 2040, 2060, 2080, and 2100, respectively. In comparison to the current 2020s scenario, the increase under SSP5-8.5 will be 3%, 6%, 9%, and 12%, respectively (Table 5). As a result, under SSP5-8.5, annual ETo will increase by 0.15 mm per year from 2020 to 2100 (Table 5).

Table 5. Daily ETo (average, range, difference, and change) for 2040, 2060, 2080, and 2100 under SSP2-4.5 and SSP5-8.5 using data from the four CMIP6 climate models, with current condition (2020) for the 13 stations.

		ETo (mm/day)				
		Current (2020)	2040	2060	2080	2100
SSP2-4.5	Average	5.71	5.8	5.9	6.0	6.1
	Range	3.7–6.9	3.6–7.0	3.7–7.2	3.7–7.2	3.7–7.4
	Δ T	-	0.1	0.2	0.28	0.35
	Change (%)	-	2	4	5	6
SSP5-8.5	Average	5.71	5.9	6.0	6.2	6.4
	Range	3.7–6.9	3.6–7.5	3.7–7.7	3.8–8.0	3.9–8.2
	Δ T	-	0.2	0.3	0.5	0.7
	Change (%)	-	3	6	9	12

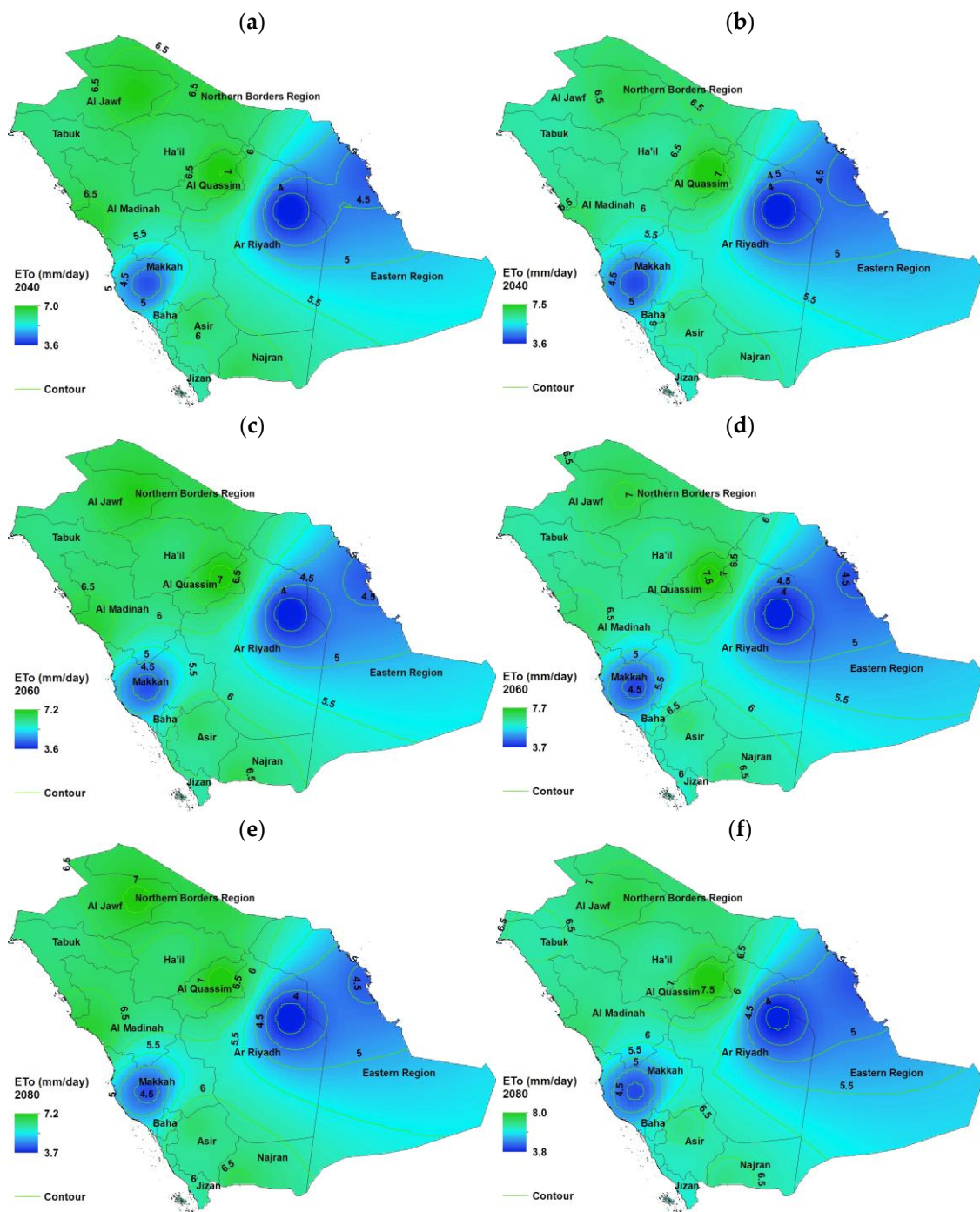


Figure 6. Cont.

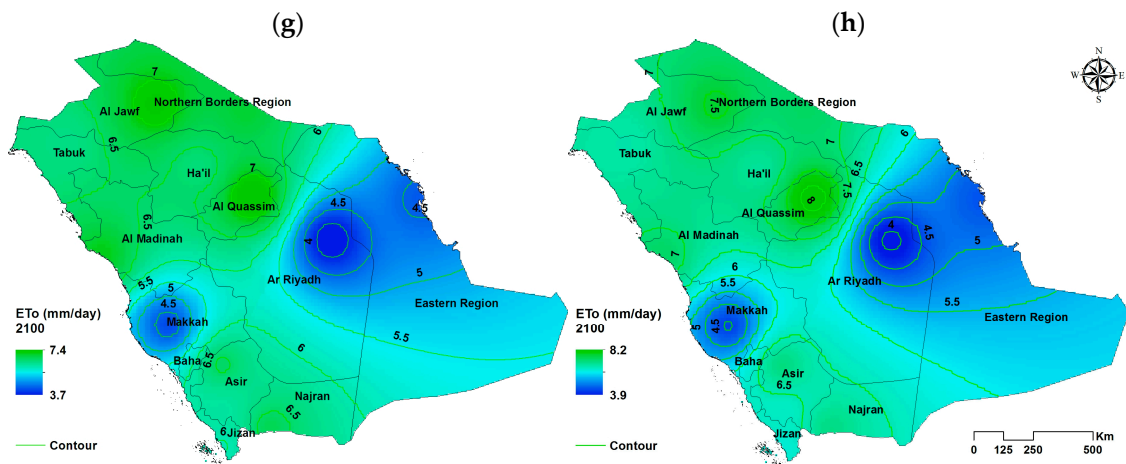


Figure 6. Annual-averaged ETo (mm/day) under SSP2-4.5 on the left for (a) 2040, (c) 2060, (e) 2080, and (g) 2100 and SSP2-8.5 on the right for (b) 2040, (d) 2060, (f) 2080, and (h) 2100, using average data from the four CMIP6 climate models.

Figure 7 shows ETo (mm) variation currently and for the SSP2-4.5 and SSP5-8.5 models for 2040, 2060, 2080, and 2100 for the 13 stations. The expected Tmax and Tmin values have increased, resulting in an upward trend in future ETo values as calculated by the CROPWAT model. This rising tendency in future ETo will result in higher crop irrigation water requirements in the future. As indicated in Figure 7, the regions with the highest ETo values will be Al Quassim, Al Jawf, Ha'il, Al Madinah, Northern region, Najran, Baha, and Tabuk, based on the findings of all SSP scenarios.

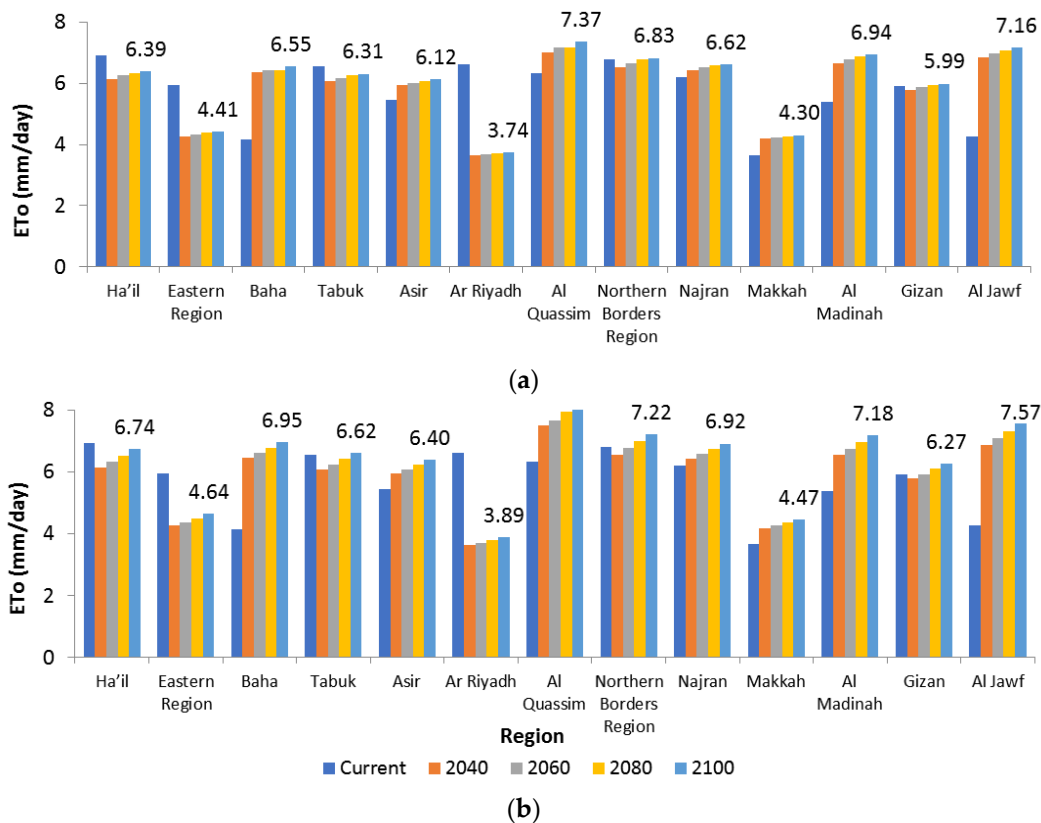


Figure 7. Estimated annual-averaged ETo (mm) under SSP2-4.5 (a) and SSP5-8.5 (b) for 2040, 2060, 2080, and 2100, using average data from the four CMIP6 climate models and the current 2020 data.

3.3. Irrigation Water Demand in Al Quassim Region

3.3.1. Simulation of Tmin, Tmax, and Rainfall

Figures 8 and 9 illustrate a box plot of the annual-averaged Tmin and Tmax under various emission scenarios projected using the four climate models (see Table 1). The results demonstrate how Tmax varies over time under SSP2-4.5, with the median being highest at 32 °C in 2060 and rising to 33.2 °C in 2100. This is consistent with SSP2-4.5 expectations, which state that greenhouse gas emissions must be under control by the year 2100. The projected mean monthly Tmin and Tmax for the 2020s, 2040s, 2060s, 2080s, and 2100s under the RCP5-8.5 scenario using the four climate models are shown in Figure A1 (Appendix A).

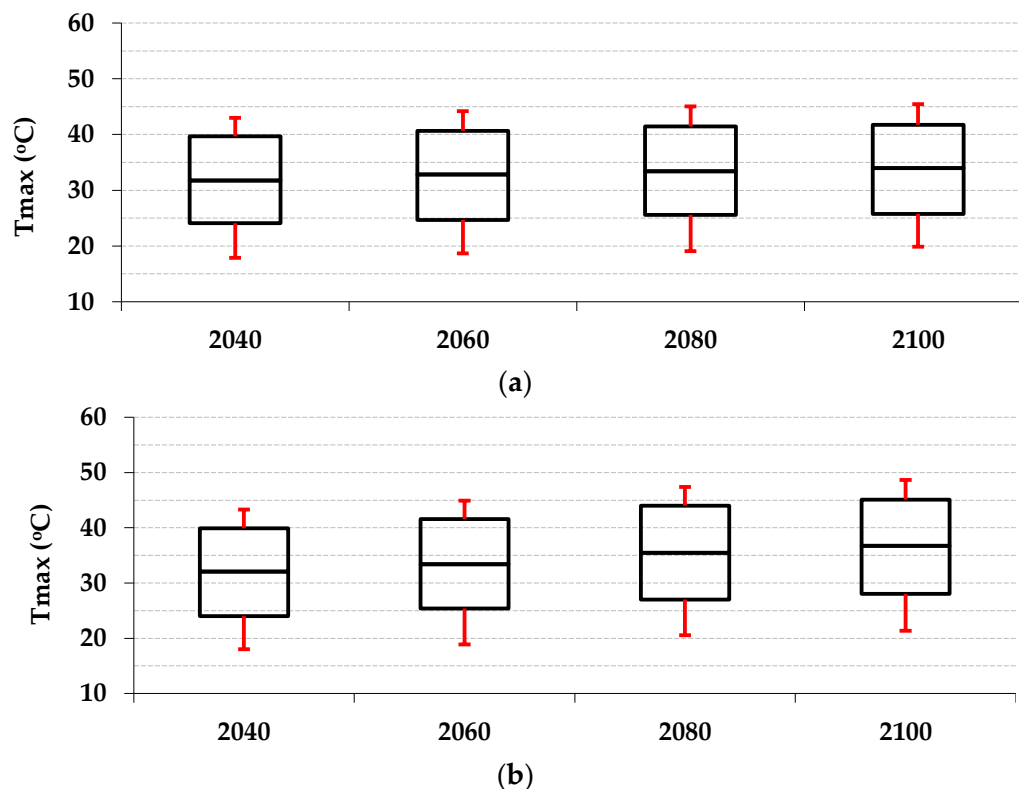


Figure 8. Box Plot of annual Tmax for four climate models under (a) SSP2-4.5 and (b) SSP5-8.5.

Figure 10 shows the variations in Tmax values between four climate scenarios for SSP2-4.5 and SSP5-8.5. For SSP2-4.5, the first climate model M1 (Table 1) predicts that Tmax will be lower in the years 2040s, 2060s, and 2080s compared to the current values while increasing by 0.33 °C in the 2100s. On the other hand, for the years 2040s, 2060s, 2080s, and 2100s, M2 and M3 have an increasing trend relative to the current Tmax. With the exception of the M1 2040s, M3 2040s, and M1 2060s, the Tmax values for the four models for SSP5-8.5 show an upward trend compared to the Tmax current value. The comparison of the four climate models (Figure 10) revealed that M1 and M3 have negative Tmax change values when compared to the other models, implying that Tmax in M1 and M3 are highly uncertain in 2040. It could be due to differences in CMIP6 climate model implementation policies and assumptions. It could also be due to the resolution (grid size), with M1 having a resolution of $1.9^{\circ} \times 1.3^{\circ}$ and M3 having $1.4^{\circ} \times 1.4^{\circ}$. M2 and M4 have resolutions of $1.1^{\circ} \times 1.1^{\circ}$ (see Table 1). Table 6 represents the computed average values for the Tmax of the four climate models.

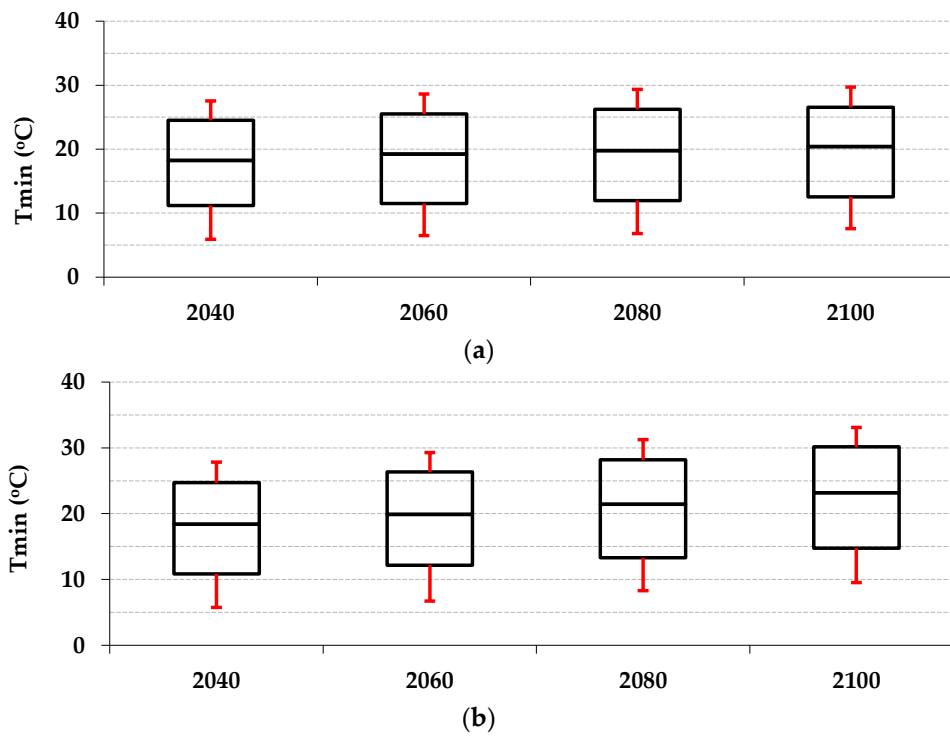


Figure 9. Box Plot of annual Tmin for four climate models under (a) SSP2-4.5 and (b) SSP5-8.5.

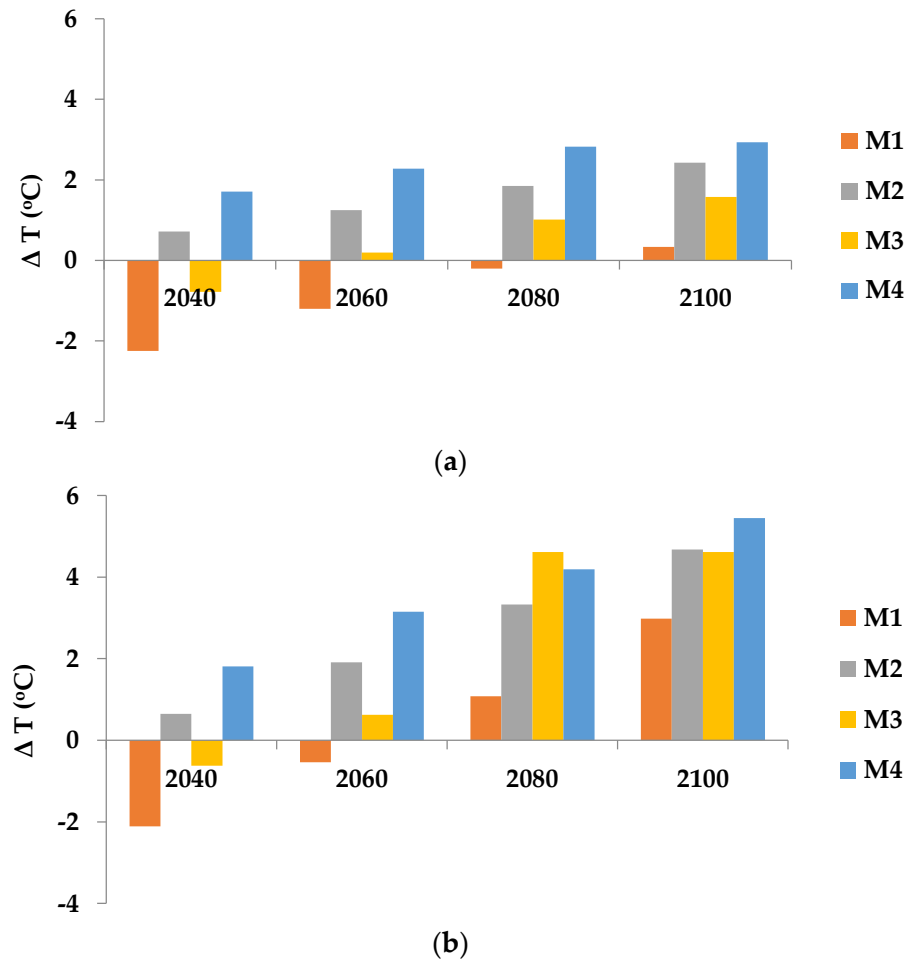


Figure 10. ΔT values for Tmax using four climate models under (a) SSP2-4.5 and (b) SSP5-8.5.

Table 6. Minimum and maximum temperatures (°C) and rainfall (mm) (average, range, difference, and change) for the 2040s, 2060s, 2080s, and 2100s under SSP2-4.5 and SSP5-8.5 using data from the four CMIP6 climate models and current conditions (2020) for the AI Quassim region.

		Min. Temp. (°C)				
		Current (2020)	2040	2060	2080	2100
SSP2-4.5	Average	16.5	17.5	18.2	18.9	19.3
	Range	6.5 (Jan.)–24.5 (Jul.)	5.9 (Jan.)–27.8 (Jul.)	6.5 (Jan.)–28.6 (Jul.)	6.8 (Jan.)–29.3 (Jul.)	7.6 (Jan.)–29.7 (Jun.)
	Δ T	-	1.0	1.7	2.3	2.8
	Change (%)	-	6.0	10.3	14.2	17.1
SSP5-8.5	Average	16.5	17.5	18.9	20.5	22.2
	Range	6.5 (Jan.)–24.5 (Jul.)	5.8 (Jan.)–27.8 (Jul.)	6.7 (Jan.)–29.3 (Jul.)	8.3 (Jan.)–31.2 (Jul.)	9.5 (Jan.)–33.1 (Jul.)
	Δ T	-	1.0	2.4	3.9	5.7
	Change (%)	-	5.9	14.4	23.9	34.3
		Max. Temp. (°C)				
SSP2-4.5	Average	31.4	31.6	32.0	32.7	33.2
	Range	18.4 (Jan.)–41.4 (Jul.)	17.9 (Jan.)–43.0 (Jun.)	18.7 (Jan.)–44.2 (Jul.)	19.0 (Jan.)–45.1 (Jul.)	22.1 (Jan.)–45.8 (Jul.)
	Δ T	-	0.2	0.6	1.4	1.8
	Change (%)	-	1	2.0	4.4	5.8
SSP5-8.5	Average	31.4	31.7	32.7	34.7	35.8
	Range	18.4 (Jan.)–41.4 (Jul.)	18.0 (Jan.)–43.3 (Jul.)	18.9 (Jan.)–44.9 (Jul.)	20.6 (Jan.)–47.4 (Jul.)	21.4 (Jan.)–48.7 (Jul.)
	Δ T	-	0.3	1.3	3.3	4.4
	Change (%)	-	1	4.1	10.5	14.1
		Rainfall (mm/day)				
SSP2-4.5	Average	5.8	7.8	7.6	7.0	7.5
	Range	0.44 (Jul.)–19.5 (Apr.)	0.3 (Jul.)–18.9 (Oct.)	0.3 (Jul.)–18.6 (Nov.)	0.2 (Jul.)–15.4 (Oct.)	0.5 (Aug.)–15.6 (Nov.)
	Δ Rainfall	-	2.0	1.8	1.2	1.7
	Change (%)	-	35.4	31.2	21.1	29.5
SSP5-8.5	Average	5.8	7.7	7.6	7.6	9.1
	Range	0.44 (Jul.)–19.5 (Apr.)	0.4 (Jul.)–20.4 (Nov.)	0.4 (Jul.)–21.6 (Nov.)	0.3 (Jul.)–18.6 (Nov.)	0.4 (Jul.)–22.9 (Sep.)
	Δ Rainfall	-	1.93	1.83	1.9	3.3
	Change (%)	-	33.1	31.7	32.2	58.0
		ETo (mm/day)				
SSP2-4.5	Average	6.3	6.3	6.5	6.5	6.6
	Range	2.8 (Jan.)–9.6 (Jul.)	2.8 (Jan.)–9.9 (Jul.)	2.9 (Jan.)–10.1 (Jul.)	2.9 (Jan.)–10.2 (Jul.)	3.0 (Jan.)–10.3 (Jul.)
	Δ Rainfall	-	0.02	0.12	0.22	0.28
	Change (%)	-	0.2	1.9	3.5	4.5
SSP5-8.5	Average	6.3	6.4	6.5	6.8	7.0
	Range	2.8 (Jan.)–9.6 (Jul.)	2.8 (Jan.)–9.9 (Jul.)	2.9 (Jan.)–10.2 (Jul.)	3.1 (Jan.)–10.5 (Jul.)	3.2 (Jan.)–10.8 (Jul.)
	Δ Rainfall	-	0.03	0.21	0.43	0.64
	Change (%)	-	0.4	3.3	6.7	10.2

Figure 11 shows the difference for the rainfall values compared to the current rainfall (ΔP) using the four climate models under SSP2-4.5 and SSP5-8.5. For SSP2-4.5 (ΔP) values for the four climate models have an increasing trend except for the M1 2080s and 2100s and the M2 2080s. SSP5-8.5 (ΔP) values for the four models have an increasing trend except for

the M1 2040s, 2060s, and 2080s and for the M2 2040s and 2080s; the average rainfall for the four models were computed in Table 6.

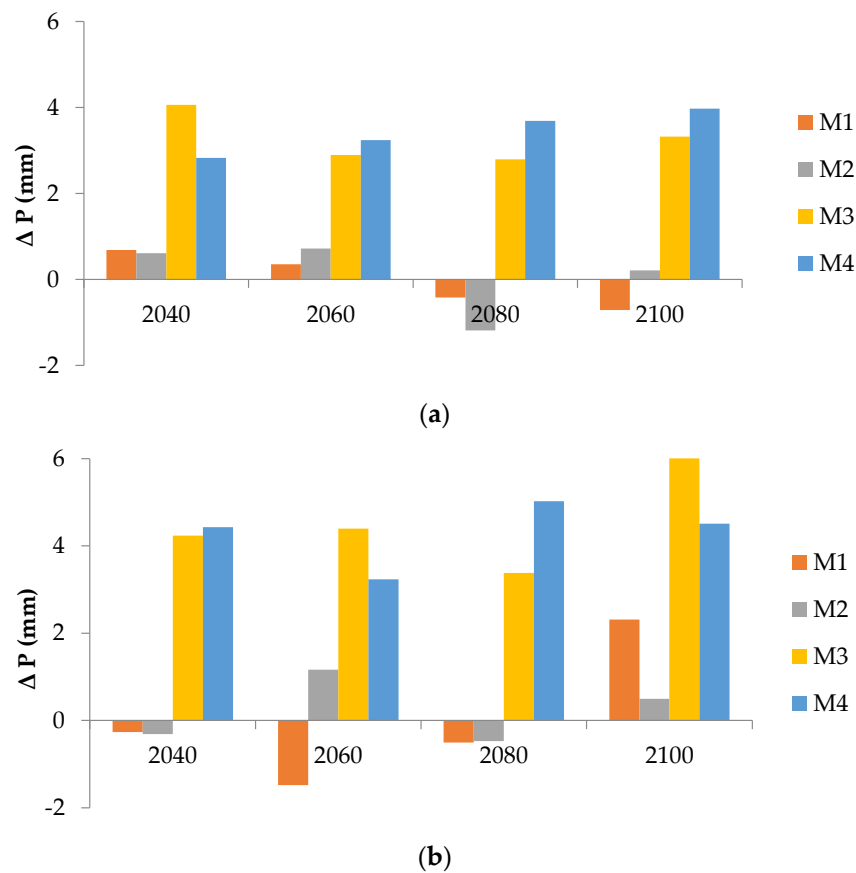


Figure 11. Δ Rainfall values for the four climate models under (a) SSP2-4.5 and (b) SSP5-8.5.

The Tmin and Tmax indicated an increasing trend for both scenarios. The results show a current mean Tmin range of 6.5 °C (in January) to 24.4 °C (in August) with an average of 16.5 °C and show a Tmax range of 18.4 °C (in January) to 41.4 °C (in July) with an average of 31.4 °C.

In 2040s, the average Tmin will rise by 1 °C under the SP2-4.5 and SSP5-8.5 scenarios, and Tmax will rise by 0.2 °C and 0.3 °C, indicating an increasing ratio of Tmin of 6.0% and 5.9% and indicating a Tmax of 1% for both scenarios. For the 2060s under the SSP2-4.5 and SSP5-8.5 scenarios, Tmin will increase by 1.7 °C and 2.4 °C, respectively, and Tmax will increase by 0.6 °C and 1.3 °C, indicating an increasing ratio for Tmin of 10% and 14% and for Tmax of 2% and 4%, respectively. For the 2080s under the SSP2-4.5 and SSP5-8.5 scenarios, Tmin will increase by 2.3 °C and 3.9 °C, and Tmax will increase by 1.4 °C and 3.3 °C, indicating an increasing ratio for Tmin of 14% and 24% and for Tmax of 4% and 11%, respectively. For the 2100s under the SSP2-4.5 and SSP5-8.5 scenarios, Tmin will increase by 2.8 °C and 5.7 °C, respectively, and Tmax will increase by 1.8 °C and 4.4 °C, indicating an increasing ratio for Tmin of 17% and 34% and for Tmax of 6% and 14%, respectively (Table 6).

The current rainfall ranged between 0.44 mm (in July) and 19.53 mm (in April) with an average value of 5.8 mm. Under SSP2-4.5 and SSP5-8.5 scenarios, the average rainfall will increase by 35.4% and 33.1%, respectively, in the 2040s. Average rainfall increases by 29.5% and 58% in the 2100s under the SSP2-4.5 and SSP5-8.5 scenarios, respectively, compared to the 2020s (Table 6).

Under the SSP2-4.5 scenario for 2020, 2040, 2060, 2080, and 2100, the average ETo will increase by 0.2%, 1.9%, 3.5%, and 4.5%, respectively, compared to the current case

(2020), while for SSP5-8.5, the average ETo will increase by 0.4%, 3.3%, 6.7%, and 10.2%, respectively (Table 6).

3.3.2. Crop Water Requirement for Al Quassim Region

The CROPWAT 8.0 model was used to predict crop water requirements (CWR) or ETc computed from Equation (2), NIWR computed from Equation (3), and growth GIWR computed from Equation (3). These were calculated for the five major key crops (wheat, maize, vegetables, clover, and dates). Simulations were performed for the current scenario (2020), as well as the SSP2-4.5 and SSP5-8.5 scenarios for the four CMIP6 climate models (Table 1) for the years 2040, 2060, 2080, and 2100. ETc is determined by the crop coefficient during various stages of crop growth (Kc). For future CWR estimation in Al Quassim region, the crop data were added to the CROPWAT model.

Table 7 summarizes the statistical analysis for the predicted NIWR values for Al Quassim region. Therefore, the current scenario indicates an NIWR of 1327.7 MCM. On the other hand, for the SSP2-4.5 emission scenario for the 2040s for the four models M1, M2, M3, and M4 NIWR would be 1294.7, 1384.5, 1332.7, and 1406.8 MCM, respectively, with an average ± standard deviation value of 1345.7±43.8 MCM. Consequently, the NIWR increasing (+) or decreasing (−) ratios are −2.5%, 4.3%, 0.4%, and 6.0%, respectively. The computed NIWR change for the years 2060, 2080, and 2100 indicate an increase of 4%, 6.4%, and 7.8%, respectively.

Table 7. Predicted net irrigation water requirements (NIWR) values in million m³ (MCM) and changes (%) compared to current obtained from four climate models for 2040, 2060, 2080, and 2100 under SSP2-4.5 and SSP5-8.5 emission scenarios and current condition (2020) for Al Quassim region.

		SSP2-4.5								
Year		Current	M1	M2	M3	M4	Average	Standard Deviation	Maximum	Minimum
2040	NIWR (MCM)	1327.7	1294.7	1384.5	1332.7	1406.8	1354.7	43.8	1425.9	1294.7
	NIWR %		−2.5	4.3	0.4	6.0	2.0	3.3	6.0	−2.5
2060	NIWR (MCM)	1327.7	1327.6	1402.5	1366.0	1425.9	1380.5	37.3	1425.9	1327.6
	NIWR %		−0.01	5.6	2.9	7.4	4.0	2.8	7.4	−0.01
2080	NIWR (MCM)	1327.7	1368.5	1421.8	1427.1	1434.5	1431.1	37.3	1473.5	1371.2
	NIWR %		3.1	7.1	7.5	8.0	6.4	2.0	8.0	3.1
2100	NIWR (MCM)	1327.7	1371.2	1436.0	1473.5	1443.6	1431.1	37.3	1473.5	1371.2
	NIWR %		3.3	8.2	11.0	8.7	7.8	2.8	11.0	3.3
		SSP5-8.5								
Year		Current	M1	M2	M3	M4	Average	Standard Deviation	Maximum	Minimum
2040	NIWR (MCM)	1327.7	1302.7	1387.4	1332.7	1405.8	1357.2	41.4	1405.8	1302.7
	NIWR %		−1.9	4.5	0.4	5.9	2.2	3.1	5.9	−1.9
2060	NIWR (MCM)	1327.7	1346.1	1436.4	1366.0	1448.7	1399.3	44.1	1448.7	1346.1
	NIWR %		1.4	8.2	2.9	9.1	5.4	3.3	9.1	1.4
2080	NIWR (MCM)	1327.7	1390.6	1462.5	1427.1	1405.8	1421.5	27.0	1462.5	1390.6
	NIWR %		4.7	10.1	7.5	5.9	7.1	2.0	10.1	4.7
2100	NIWR (MCM)	1327.7	1439.0	1499.4	1473.5	1447.9	1465.0	23.6	1499.4	1439.0
	NIWR %		8.4	12.9	11.0	9.1	10.3	1.8	12.9	8.4

In addition, RCP 8.5 scenario for the year 2040 for the four models M1, M2, M3, and M4 indicate NIWR values of 13,024.7, 1387.4, 1332.7, and 1406.8 MCM, respectively, with an average ± standard deviation value of 1357.2±41.4 MCM and a range between 1302.7 to 1408.8 MCM. Consequently, the NIWR increasing (+) or decreasing (−) ratios are −1.9%, 4.5%, 0.4%, and 5.9%, respectively. The computed NIWR average ± standard deviation change for the years 2060, 2080, and 2100 indicate an increase of (5.4 ± 3.3), (7.1 ± 2.0), and (10.3 ± 1.8)%, respectively.

The M1 SSP2-4.5 and SSP5-8.5 negative values of NIWR in 2040 (−2.5% and −1.9%) indicate that the projected data from M1 are contrary to expectations, as indicated by other models that show an increase in greenhouse emissions. M1’s projected climate data in the 2040s seem to be uncertain.

The CROPWAT 8 output for the current scenario indicated that dates has the maximum ETc (2175 mm) and that wheat has the lowest ETc (621 mm). On the other hand, clover, maize, and other vegetables had ETc values of 1815, 975.6, and 650.2 mm, respectively. As a result, the maximum NIWR for dates was 835.3 MCM, while the lowest NIWR was 40.9 MCM for other vegetables. Wheat, clover, and maize had NIWR values of 132.9, 261, and 57.6 MCM, respectively.

This demonstrates that because wheat and other vegetables are cultivated during the winter season when temperatures are at their lowest, their resulting ETo values are lowest.

As a result, the total NIWR for all crops was 1327.7 MCM (Table 8). Based on an irrigation efficiency of 75%, the current GIWR is 1584.7. The NIWR and GIWR for the year 2040 for SSP2-4.5 are 1354.5 and 1617.7 MCM, respectively, which is a 2.5% increase over the current scenario (Table 8). Furthermore, the predicted NIWRs for the SSP2-4.5 for the 2040s, 2060s, 2080s, and 2100s are 1354.7, 1380.5, 1413.0, and 1431.1 MCM, respectively, with an increase of 2.5, 4.8, 7.8, and 9.4% compared to the current scenario 2020s. The predicted NIWRs for the SSP5-8.5 for the 2040s, 2060s, 2080s, and 2100s are 1357.2, 1399.3, 1421.5, and 1465.0 MCM, respectively, with an increase of 2.7, 6.5, 8.5, and 12.4% compared to the current scenario 2020s. Figure 12 depicts the NIWR variability.

Table 8. Averaged net irrigation water requirements (NIWR) and growth irrigation water requirements (GIWR) in million m³ (MCM) for four climate models under SSP2-4.5 and SSP5-8.5 for 2040, 2060, 2080, and 2100, with current condition (2020) for Al Quassim region.

		Year				
		Current (2020)	2040	2060	2080	2100
SSP2-4.5	NIWR (MCM)	1327.7	1354.7	1380.5	1413.0	1431.1
	GIWR (MCM) *	1584.7	1617.7	1648.6	1687.6	1708.9
	GIWR Change (%)	-	2.5	4.8	7.8	9.4
SSP5-8.5	NIWR (MCM)	1327.7	1357.2	1399.3	1421.5	1465.0
	GIWR (MCM) *	1584.7	1620.6	1670.6	1697.5	1749.2
	GIWR Change (%)	-	2.7	6.5	8.5	12.4

Notes: NIWR, net irrigation water requirement; MCM, million m³; and GIWR, growth irrigation water requirements. * Sprinkler irrigation system for wheat, clover, other vegetables, maize, tomato, and potato (Irrigation efficiency 75%) and drip irrigation system for dates and citrus (Irrigation efficiency 90%) [46].

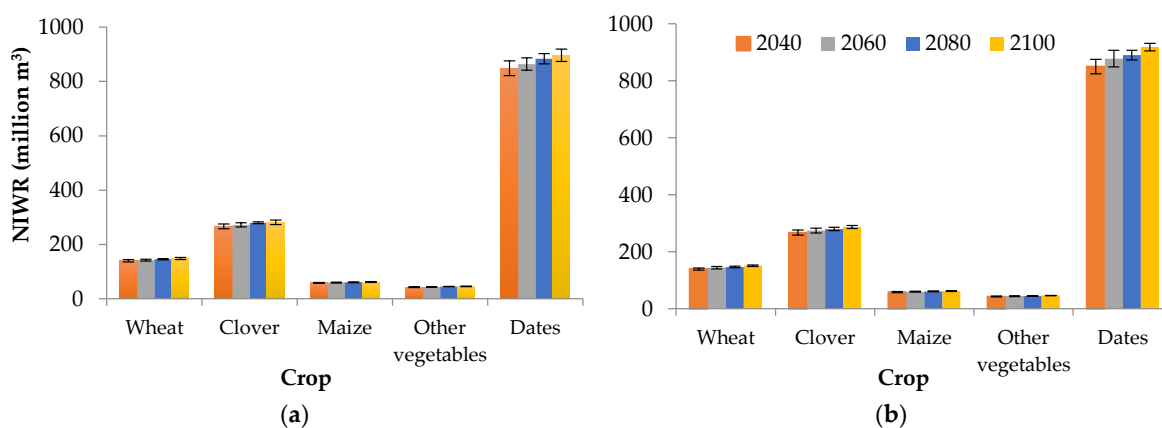


Figure 12. NIWR (net irrigation water requirement) variability in Al Quassim region for five crops and four climate models (indicated by error bar) for 2040, 2060, 2080, and 2100 under (a) SSP2-4.5 and (b) SSP5-8.5.

4. Discussion

According to the findings above, climate change will have a massive effect on Saudi Arabia's agricultural irrigation water requirements in the future. The Al Quassim region is considered as a case study for the impact of climate change on agricultural irrigation water demands in Saudi Arabia. According to the findings, both temperature and rainfall will increase for the 13 climate stations under both SSPs scenarios, with average data of the four CMIP6 climate models, with the SSP5-8.5 scenario showing the greatest increase.

Comparing the results of the temperature and rainfall changes of this study with the literature, there is a good match with Almazroui et al. [39] as they studied the climate change impacts on the Arabian Peninsula using 31 CMIP6 models. They came to the conclusion that the variations were found by investigating the 31 CMIP6 models for the 2030–2059 and 2070–2099 future periods, with comparison to the base case 1981–2010, under three future SSPs. They discovered that under SPP2-4.5 and SSP5-8.5 scenarios, the temperature is anticipated to rise by 1.74 and 2.17 °C in 2060, respectively, while in 2100 the temperature is expected to rise by 2.87 and 5.28 °C, respectively, compared to the base case. On the other hand, Almazroui et al. [39] concluded that under all SSPs scenarios the annual mean rainfall averaged over Saudi Arabia has an increase of 3.76–31.83% by the end of the 2100s. As a result, the current study's results agree with those predicted by Almazroui et al. [39].

The two SSPs scenarios resulted in an increase in ETo. Chowdhury et al. [4] examined the effects of climate change on CWRs from 2011 to 2050 in the Al-Jouf region. They observed that a 1 °C rise in temperature could increase the overall CWR by 2.9% in this region. The increase in CWR has been calculated to be 1.5 MCM/year since 2011, which is equal to a CWR producing roughly 600 tons of wheat per year on a linear trend. The CWR increased mostly as a result of rising temperatures, with changes in rainfall having little impact.

Tarawneh and Chowdhury [23] investigated forecasted temperature and rainfall trends in various Saudi Arabian areas. According to all emission scenarios, temperatures increased in all locations from 1986 to 2005. RCP8.5 predicts temperature rises of 0.8–1.6 °C, 0.9–2.7 °C, and 0.7–4.1 °C for the years 2025–2044, 2045–2064, and 2065–2084, respectively. On the other hand, rainfall patterns varied depending on the emission scenarios and time periods studied. The RCP6 showed a decrease in rainfall from the reference period in most regions, while the RCP8.5 and RCP2.6 showed a variety of patterns. Long-term water resource management plans may become more difficult to develop as temperatures rise and rainfall patterns become more erratic. However, the current study's findings are consistent with those predicted in the RCP8.5 scenario by Tarawneh and Chowdhury [23].

The impacts of future temperature variations in the Al Quassim region were investigated in this study. Under SSP2-4.5, the results suggest that the planned development of Al Quassim is viable until 2100 with the available land and groundwater resources. Adjustments in land distribution are required in the more severe SSP5-8.5 emission scenario to supply the requisite crop acreage for population and livestock agricultural needs through 2100. These findings are based on assumptions including current population and animal water needs, current crop demand, and a population growth rate of 2.5%. Furthermore, more water may be needed in the future to compensate for potential groundwater shortages and soil salinity.

Unless more water sources would become available to mitigate the effects of climatic changes in the study area, the parts of cropped areas affected by water deficits will be 6.1% for wheat, 2.9% for clover, 1.4% for maize, 5.3% for other vegetables, and 2.5% for dates in 2040 under SSP5-4.5, as shown in Figure 13. There are higher deficits in 2100 under SSP5-8.5, with values of 15.1%, 10.7%, 8.3%, 13.9%, and 10.7%, respectively. These findings indicate that, while climate models have inherent uncertainty in their forecasts, climate change has a clear impact on agricultural productivity in the Al Quassim region. As a result, climate change has a significant impact on agricultural planning and management. To improve management of the available water resources, increased irrigation efficiency

with intelligent irrigation technologies [47,48], strategic crop planting, or crop patterns that use the less irrigation water can all assist in mitigating the future impact of climate change on water irrigation requirements in the Al Quassim region.

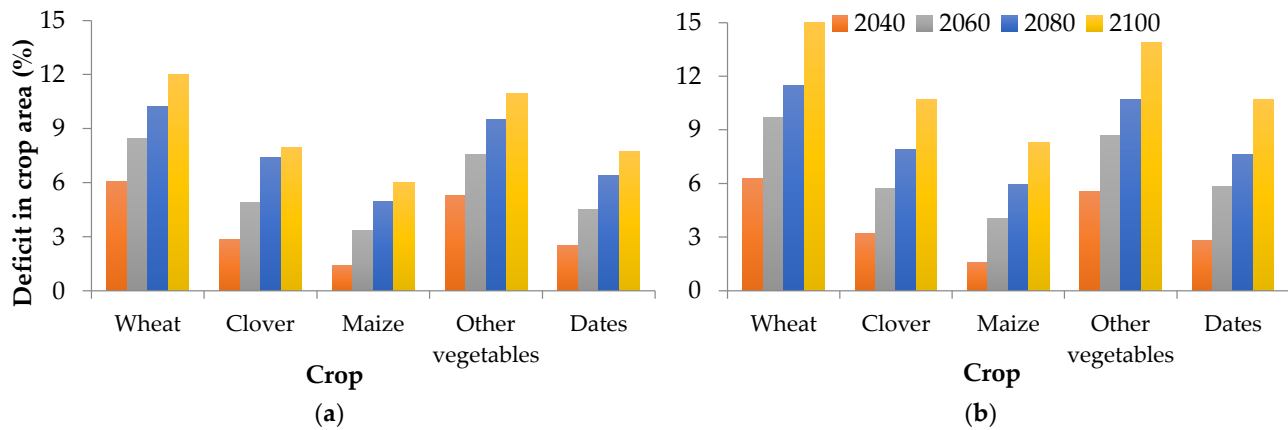


Figure 13. Deficit in crop areas (%) in Al Quassim region for 2040, 2060, 2080, and 2100: (a) SSP2-4.5 and (b) SSP5-8.5.

5. Conclusions

Climate change represents one of the most challenging environmental issues confronting development, especially in arid and semi-arid regions. Different meteorological data were downloaded from the CMIP6 database under four climate models with two emission scenarios: SSP2-4.5 and SSP5-8.5. This study analyzed annual-averaged Tmax, Tmin, rainfall, and ETo distribution maps in Saudi Arabia for the 2020s using weather data from 13 stations (Al Jawf, Baha, Eastern Province, Al Quassim, Gizan, Northern Frontier, Ha'il, Al Madinah, Najran, Ar Riyadh, Asir, Tabuk, and Makkah). Moreover, SSP2-4.5 and SSP5-8.5 scenarios in the 2040s, 2060s, 2080s, and 2100s utilizing the future climatic parameters predicted using four CMIP6 climate models as input data for the CROPWAT 8.0 model to compute ETo and effective rainfall were involved.

The comparison of the four climate models revealed that M1 predicted climate data with values in 2040 were lower than the current case under both SSP2-4.5 and SSP5-8.5 scenarios.

The findings revealed that the expected temperature values had an increasing tendency in the future. As a result, the rising trend of ETo will result in increased crop irrigation water requirements. All SSPs scenarios showed that Al Quassim, Al Jawf, Ha'il, Al Madinah, Northern region, Najran, Baha, and Tabuk have the highest ETo values in Saudi Arabia.

The anticipated future irrigation demands for the Al Quassim region under a changing climate scenario reveal net irrigation water demands greater than the SSP2-4.5 scenario by 2040, 2060, 2080, and 2100.

The greater demand estimated for the Al Quassim region under the SSP5-8.5 scenario were due to the SSP5-8.5 scenario's showed higher temperature values compared to the SSP2-4.5 scenario. Moreover, the average crop irrigation demands for wheat, maize, various vegetables, clover, and dates were lower in the SSP2-4.5 scenario than in the SSP5-8.5 scenario.

As a conclusion, more water will be needed to address any expected increase in ETo to maintain the increased irrigation water requirements in the future. This study could be useful to help planners and policymakers to identify adaptation strategies for similar climatic regions in order to mitigate the effects of climate change. These monitoring and management strategies could help in the long run to reduce and minimize the expected adverse effects of climate change in the study area. These include the use of more advanced irrigation techniques, the reduction of exploitation/controlled pumping, and the construction of multifunctional dams and trenches along with artificial recharging through surface

water from pond, trench, and wells help to prevent or at least minimize upcoming and lateral migration of saline groundwater.

Author Contributions: Conceptualization, M.E.-R.; methodology, M.E.-R., M.E.G. and O.B.; software, M.E.-R. and M.E.G.; validation, M.E.-R.; formal analysis, M.E.-R.; investigation, M.E.-R.; resources, M.E.-R.; data curation, M.E.-R.; writing—original draft preparation, M.E.-R. and M.E.G.; writing—review and editing, M.E.-R., M.E.G., O.B., A.A., F.A. and N.A.-A.; visualization, M.E.-R. All authors have read and agreed to the published version of the manuscript.

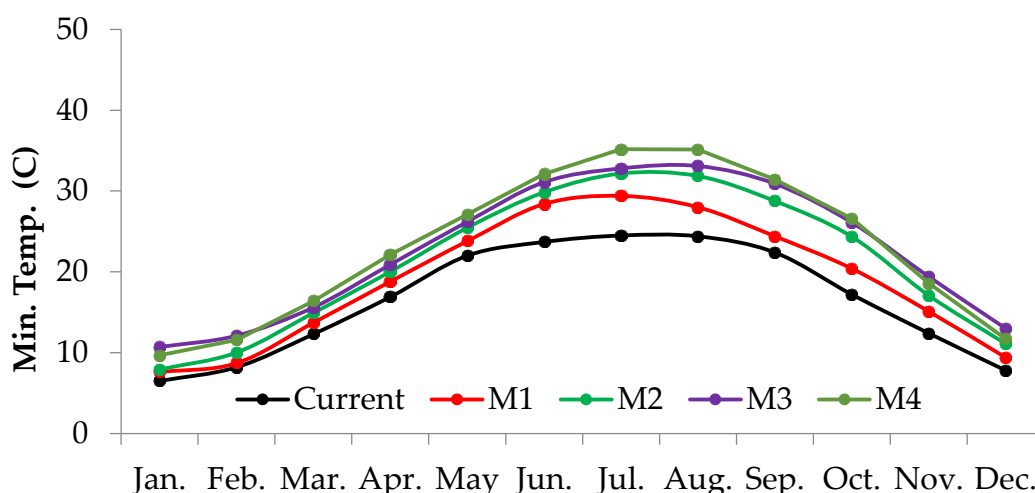
Funding: This research received no external funding.

Data Availability Statement: Data available based on request from first author.

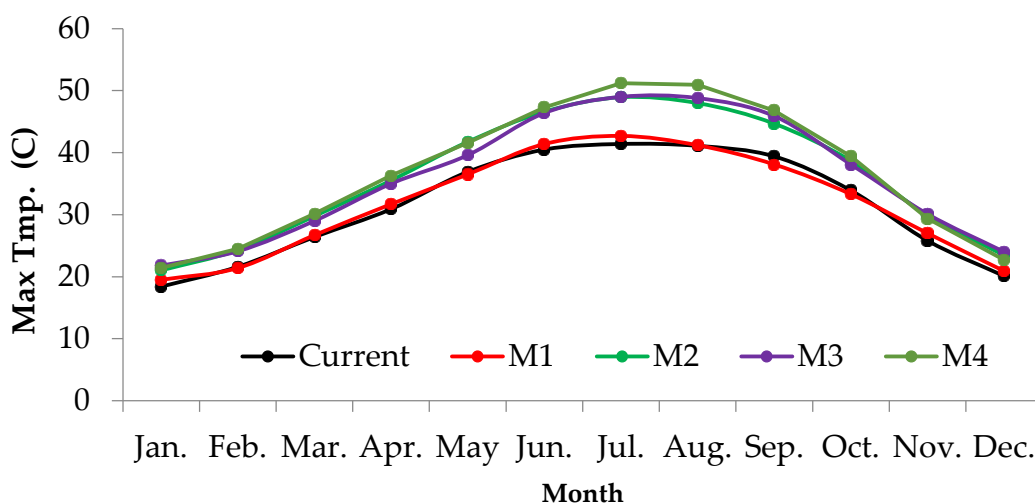
Acknowledgments: The authors acknowledge the World Climate Research Programme, which oversees the Coupled Model Intercomparison Project–Phase 6 (CMIP6), for providing the climate data used in this study. Al-Arifi thanks the Deanship of Scientific Research, King Saud University for funding through Vice Deanship of Scientific Research Chairs. The authors also thank the journal editor and two other anonymous reviewers for their valuable comments and suggestions.

Conflicts of Interest: The authors declare no conflict of interest.

Appendix A



(a)



(b)

Figure A1. (a) Tmin and (b) Tmax for four climate models under SSP5-8.5.

References

- Masia, S.; Trabucco, A.; Spano, D.; Snyder, R.L.; Sušnik, J.; Marras, S. A modelling platform for climate change impact on local and regional crop water requirements. *Agric. Water Manag.* **2021**, *255*, 107005. [CrossRef]
- Gabr, M.E.S. Management of irrigation requirements using FAO-CROPWAT 8.0 model: A case study of Egypt. *Model. Earth Syst. Environ.* **2022**, *8*, 3127–3142. [CrossRef]
- Gabr, M.E.S. Modelling net irrigation water requirements using FAO-CROPWAT 8.0 and CLIMWAT 2.0: A case study of Tina Plain and East South ElKantara regions, North Sinai Egypt. *Arch. Agron. Soil Sci.* **2021**, *68*, 1322–1337. [CrossRef]
- Chowdhury, S.; Al-Zahrani, M.; Abbas, A. Implications of climate change on crop water requirements in arid region: An example of Al-Jouf, Saudi Arabia. *J. King Saud Univ. Eng. Sci.* **2016**, *28*, 21–31. [CrossRef]
- Eyring, V.; Bony, S.; Meehl, G.A.; Senior, C.A.; Stevens, B.; Stouffer, R.J.; Taylor, K.E. Overview of the Coupled Model Intercomparison Project Phase 6 (CMIP6) experimental design and organization. *Geosci. Model Dev.* **2016**, *9*, 1937–1958. [CrossRef]
- Meehl, G.A.; Covey, C.; Delworth, T.; Latif, M.; McAvaney, B.; Mitchell, J.F.B.; Stouffer, R.J.; Taylor, K.E. The WCRP CMIP3 multimodel dataset: A new era in climatic change research. *Bull. Am. Meteorol. Soc.* **2007**, *88*, 1383–1394. [CrossRef]
- Taylor, K.E.; Stouffer, R.J.; Meehl, G.A. An overview of CMIP5 and the experiment design. *Bull. Am. Meteorol. Soc.* **2012**, *93*, 485–498. [CrossRef]
- Ogata, T.; Ueda, H.; Inoue, T.; Hayasaki, M.; Yoshida, A.; Watanabe, S.; Kumai, A. Projected future changes in the Asian monsoon: A comparison of CMIP3 and CMIP5 model results. *J. Meteorol. Soc. Japan. Ser. II* **2014**, *92*, 207–225. [CrossRef]
- Core Writing Team; Pachauri, R.K.; Meyer, L.A. (Eds.) *IPCC: Climate Change 2014: Synthesis Report. Contribution of Working Groups I, II and III to the Fifth Assessment Report of the Intergovernmental Panel on Climate Change*; IPCC: Geneva, Switzerland, 2014; p. 151. Available online: https://ar5-syr.ipcc.ch/ipcc/ipcc/resources/pdf/IPCC_SynthesisReport.pdf (accessed on 16 December 2022).
- Bouras, E.; Jarlan, L.; Khabba, S.; Er-Raki, S.; Dezetter, A.; Sghir, F.; Tramblay, Y. Assessing the impact of global climate changes on irrigated wheat yields and water requirements in a semi-arid environment of Morocco. *Sci. Rep.* **2019**, *9*, 1–14. [CrossRef]
- Zhang, Y.; You, Q.; Chen, C.; Ge, J. Impacts of climate change on streamflows under RCP scenarios: A case study in Xin River Basin, China. *Atmos. Res.* **2016**, *178*, 521–534. [CrossRef]
- Allani, M.; Mezzi, R.; Zouabi, A.; Béji, R.; Joumade-Mansouri, F.; Hamza, M.E.; Sahli, A. Impact of future climate change on water supply and irrigation demand in a small Mediterranean catchment. Case study: Nebhana dam system, Tunisia. *J. Water Clim. Chang.* **2020**, *11*, 1724–1747. [CrossRef]
- Zamani, Y.; Hashemi Monfared, S.A.; Hamidianpour, M. A comparison of CMIP6 and CMIP5 projections for precipitation to observational data: The case of Northeastern Iran. *Theor. Appl. Climatol.* **2020**, *142*, 1613–1623. [CrossRef]
- Eyring, V.; Cox, P.M.; Flato, G.M.; Gleckler, P.J.; Abramowitz, G.; Caldwell, P.; Williamson, M.S. Taking climate model evaluation to the next level. *Nat. Clim. Chang.* **2019**, *9*, 102–110. [CrossRef]
- Van Vuuren, D.P.; Riahi, K. The relationship between short-term emissions and long-term concentration targets. *Clim. Chang.* **2011**, *104*, 793–801. [CrossRef]
- Gusain, A.; Ghosh, S.; Karmakar, S. Added value of CMIP6 over CMIP5 models in simulating Indian summer monsoon rainfall. *Atmos. Res.* **2020**, *232*, 104680. [CrossRef]
- Nie, S.; Fu, S.; Cao, W.; Jia, X. Comparison of monthly air and land surface temperature extremes simulated using CMIP5 and CMIP6 versions of the Beijing Climate Center climate model. *Theor. Appl. Climatol.* **2020**, *140*, 487–502. [CrossRef]
- Rivera, J.A.; Arnould, G. Evaluation of the ability of CMIP6 models to simulate precipitation over Southwestern South America: Climatic features and long-term trends (1901–2014). *Atmos. Res.* **2020**, *241*, 104953. [CrossRef]
- Kamruzzaman, M.; Shahid, S.; Islam, A.R.M.; Hwang, S.; Cho, J.; Zaman, M.; Hossain, M. Comparison of CMIP6 and CMIP5 model performance in simulating historical precipitation and temperature in Bangladesh: A preliminary study. *Theor. Appl. Climatol.* **2021**, *145*, 1385–1406. [CrossRef]
- Gurara, M.A.; Jilo, N.B.; Tolche, A.D. Impact of climate change on potential evapotranspiration and crop water requirement in Upper Wabe Bridge watershed, Wabe Shebele River Basin, Ethiopia. *J. Afr. Earth Sci.* **2021**, *180*, 104223. [CrossRef]
- Mojid, M.A.; Rannu, R.P.; Karim, N.N. Climate change impacts on reference crop evapotranspiration in North-West hydrological region of Bangladesh. *Int. J. Climatol.* **2015**, *35*, 4041–4046. [CrossRef]
- Zhou, T.; Wu, P.; Sun, S.; Li, X.; Wang, Y.; Luan, X. Impact of future climate change on regional crop water requirement—A case study of Hetao Irrigation District, China. *Water* **2017**, *9*, 429. [CrossRef]
- Tarawneh, Q.Y.; Chowdhury, S. Trends of climate change in Saudi Arabia: Implications on water resources. *Climate* **2018**, *6*, 8. [CrossRef]
- Moghazy, N.H.; Kaluarachchi, J.J. Impact of Climate Change on Agricultural Development in a Closed Groundwater-Driven Basin: A Case Study of the Siwa Region, Western Desert of Egypt. *Sustainability* **2021**, *13*, 1578. [CrossRef]
- Abdrabbo, M.A.; Farag, A.A.; El-Desokey, W.M.S. Implementing of RCPs scenarios for the prediction of evapotranspiration in Egypt. *Int. J. Plant Soil Sci.* **2015**, *6*, 50–63. [CrossRef]
- Allen, R.G.; Pereira, L.S.; Raes, D.; Smith, M. Crop evapotranspiration—Guidelines for computing crop water requirements—FAO Irrigation and drainage paper 56. *Fao Rome* **1998**, *300*, D05109.
- Yassen, A.N.; Nam, W.H. Climate Change Impacts on Reference Evapotranspiration and Drought Risk Management under Environmental Egyptian Condition. Master's Thesis, Hankyong National University, Anseong, Republic of Korea, 2018; p. 296.

28. Salama, M.A.; Yousef, K.M.; Mostafa, A.Z. Simple equation for estimating actual evapotranspiration using heat units for wheat in arid regions. *J. Radiat. Res. Appl. Sci.* **2015**, *8*, 418–427. [CrossRef]
29. El-Nashar, W.Y.; Hussien, E.A. Estimating the potential evapo-transpiration and crop coefficient from climatic data in Middle Delta of Egypt. *Alex. Eng. J.* **2013**, *52*, 35–42. [CrossRef]
30. Smith, M. *CROPWAT: A Computer Program for Irrigation Planning and Management (No. 46)*; Food and Agriculture Organization of the United Nations: Italy, Rome, 1992; Available online: <https://www.fao.org/land-water/databases-and-software/cropwat/en/> (accessed on 15 February 2022).
31. FAO. AquaCrop. 2022. Available online: <https://www.fao.org/aquacrop/en/> (accessed on 8 December 2022).
32. Climate Change Knowledge Portal (CCKP). Current Climate Climatology in Saudi Arabia. Available online: <https://climateknowledgeportal.worldbank.org/country/saudi-arabia/climate-data-historical> (accessed on 20 January 2022).
33. Baig, M.B.; Alotibi, Y.; Straquadine, G.S.; Alataway, A. Water Resources in the Kingdom of Saudi Arabia: Challenges and Strategies for Improvement. In *Water Policies in MENA Countries*; Zekri, S., Ed.; Global Issues in Water Policy; Springer: Cham, Switzerland, 2020; pp. 135–160.
34. Ministry of Agriculture and Water (MAW). *Water Atlas of Saudi Arabia*; Ministry of Agriculture and Water (MAW): Ar Riyadh, Saudi Arabia, 1984.
35. Alkolibi, F.M. Possible Effects of Global Warming on Agriculture and Water Resources in Saudi Arabia: Impacts and Responses. *Clim. Chang.* **2002**, *54*, 225–245. [CrossRef]
36. Chowdhury, S.; Al-Zahrani, M. Water resources and water consumption pattern in Saudi Arabia. In Proceedings of the 10th Gulf Water Conference, At Doha, Qatar, 22–24 April 2012.
37. Al-Sheikh, H.M. Appendix 8: Country Case Study-Water policy Reform in Saudi Arabia. In Proceedings of the Second Expert Consultation on National Water Policy Reform in the Near East, Cairo, Egypt, 24–25 November 1997.
38. Al-Salamah, I.S.; Ghazaw, Y.M.; Ghumman, A.R. Groundwater modeling of Saq Aquifer Buraydah Al Qassim for better water management strategies. *Environ. Monit. Assess.* **2011**, *173*, 851–860. [CrossRef]
39. Almazroui, M.; Saeed, S.; Saeed, F.; Islam, M.N.; Ismail, M. Projections of precipitation and temperature over the South Asian countries in CMIP6. *Earth. Syst. Environ.* **2020**, *4*, 297–320. [CrossRef]
40. Bi, D.; Dix, M.; Marsland, S.; O’Farrell, S.; Rashid, H.; Uotila, P.; Puri, K. The ACCESS coupled model: Description, control climate and evaluation. *Aust. Meteorol. Oceanogr. J.* **2013**, *63*, 41–64. [CrossRef]
41. Wu, T.; Lu, Y.; Fang, Y.; Xin, X.; Li, L.; Li, W.; Liu, X. The Beijing Climate Center climate system model (BCC-CSM): The main progress from CMIP5 to CMIP6. *Geosci. Model Dev.* **2019**, *12*, 1573–1600. [CrossRef]
42. Voldoire, A.; Saint-Martin, D.; Sénési, S.; Decharme, B.; Alias, A.; Chevallier, M.; Waldman, R. Evaluation of CMIP6 DECK experiments with CNRM-CM6-1. *J. Advan. Model Earth Syst.* **2019**, *11*, 2177–2213. [CrossRef]
43. Yukimoto, S.; Kawai, H.; Koshiro, T.; Oshima, N.; Yoshida, K.; Urakawa, S.; Ishii, M. The Meteorological Research Institute Earth System Model version 2.0, MRI-ESM2.0: Description and basic evaluation of the physical component. *J. Meteor. Soc. Jpn. Ser. II* **2019**, *97*, 931–965. [CrossRef]
44. General Authority of Statistics. *Statistical Year Book for 2012*; General Authority of Statistics: Saudi Arabia, Ar Riyadh, 2012.
45. Ministry of Environment, Water and Agriculture (MEWR). *Statistical Reports—2020*. Saudi Arabia. Available online: <https://rb.gy/m4j0ha> (accessed on 20 January 2022).
46. Brouwn, C.; Prins, K.; Heibloem, M. *Irrigation Water Management: Irrigation Scheduling Training Manual, No 4*; Food and Agriculture Organization: Rome, Italy, 1989.
47. Al-Ghobari, H.M.; Mohammad, F.S. Intelligent irrigation performance: Evaluation and quantifying its ability for conserving water in arid region. *App. Water Sci.* **2011**, *1*, 73–83. [CrossRef]
48. El-Rawy, M.; Haraz, O.M.; Morsy, M.A.; Saad, W. Role of smart technology to increase date productivity and water efficiency in MENA countries: A review of innovative sustainable solutions. *Euro-Mediterr. J. Environ. Integr.* **2021**, *6*, 1–11. [CrossRef]

Disclaimer/Publisher’s Note: The statements, opinions and data contained in all publications are solely those of the individual author(s) and contributor(s) and not of MDPI and/or the editor(s). MDPI and/or the editor(s) disclaim responsibility for any injury to people or property resulting from any ideas, methods, instructions or products referred to in the content.